Mesh Hydrodynamics Results

Mladen Ivkovic

Laboratory of Astrophysics
École Polytechnique Fédérale de Lausanne

March 3, 2020

Contents

1 Notation **3**

2 Advection **4**
2.1 Piecewise Constant . . . 4
2.2 Piecewise Linear . . . 14
2.3 Order of Convergence . . . 22
2.4 Conclusions . . . 27
2.5 Future Debugging Hints . . . 32
2.5.1 When you're using downwind differencing . . . 32
2.5.2 When the CFL condition is violated . . . 38

3 Slope and Flux Limiters **43**
3.1 Slope Limiters . . . 43
3.1.1 What slope limiters have in common . . . 45
3.1.2 Effects on linear advection . . . 48

4 Riemann Solvers **50**
4.1 Approximate Riemann Solutions . . . 50
4.2 Conclusions . . . 53

5 Godunov's Method **54**
5.1 Solving Riemann Problems using Godunov's Method . . . 54
5.2 Solving Vacuum Riemann Problems using Godunov's Method . . . 56
5.3 Order of Convergence Study . . . 56
5.4 Conclusions . . . 58

1 Notation

We are working on numerical methods. Both space and time will be discretized.

Space will be discretized in cells which will have integer indices to describe their position. Time will be discretized in fixed time steps, which may have variable lengths. Nevertheless the time progresses step by step.

The lower left corner has indices $(0, 0)$ in 2D. In 1D, index 0 also represents the leftmost cell.

We have:

- integer subscript: Value of a quantity at the cell, i.e. the center of the cell. Example: $\mathbf{U}_i$, $\mathbf{U}_{i-2}$ or $\mathbf{U}_{i,j+1}$ for 2D.
- non-integer subscript: Value at the cell faces, e.g. $\mathbf{F}_{i-1/2}$ is the flux at the interface between cell i and $i-1$, i.e. the left cell as seen from cell i.
- integer superscript: Indication of the time step. E.g. $\mathbf{U}^n$: State at timestep n
- non-integer superscript: (Estimated) value of a quantity in between timesteps. E.g. $\mathbf{F}^{n+1/2}$: The flux at the middle of the time between steps n and $n+1$.

2 Advection

2.1 Piecewise Constant

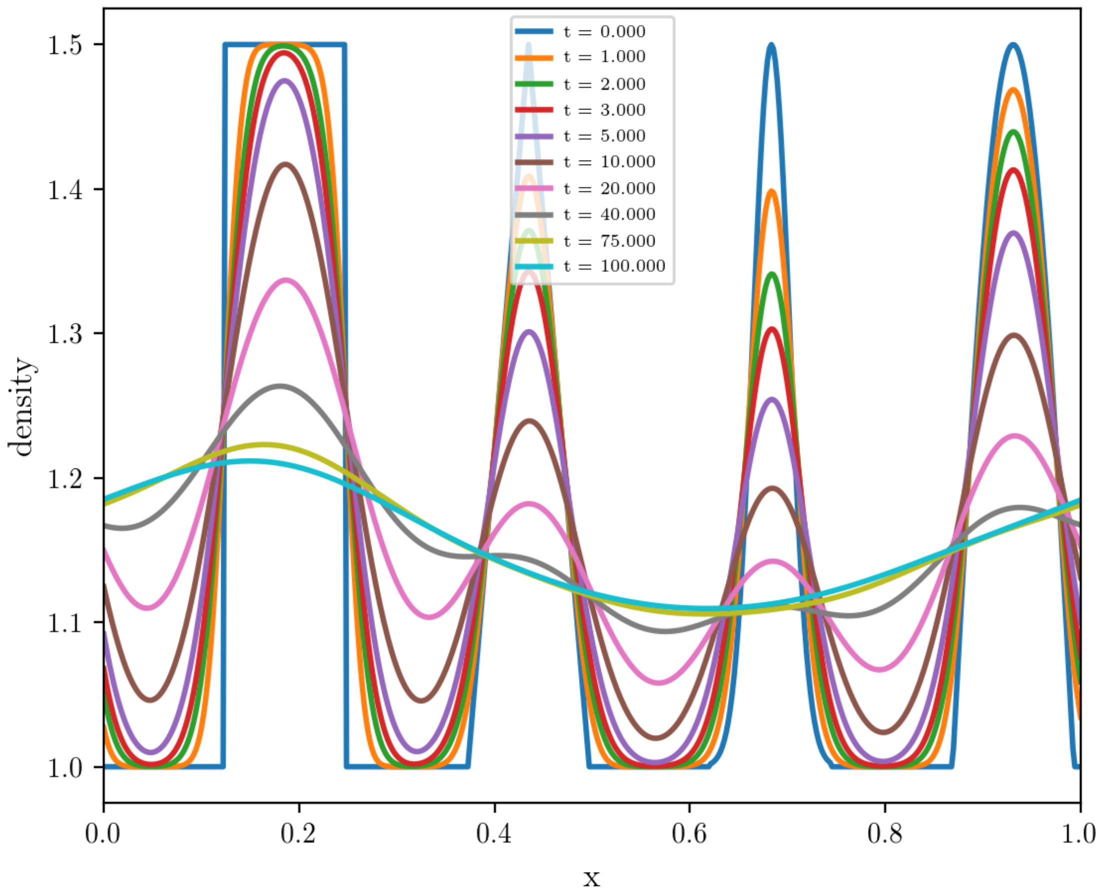

Figure 1: Piecewise constant advection with positive fixed global velocity $v_x = 1$. $C_{CFL} = 0.9$, $nx = 500$

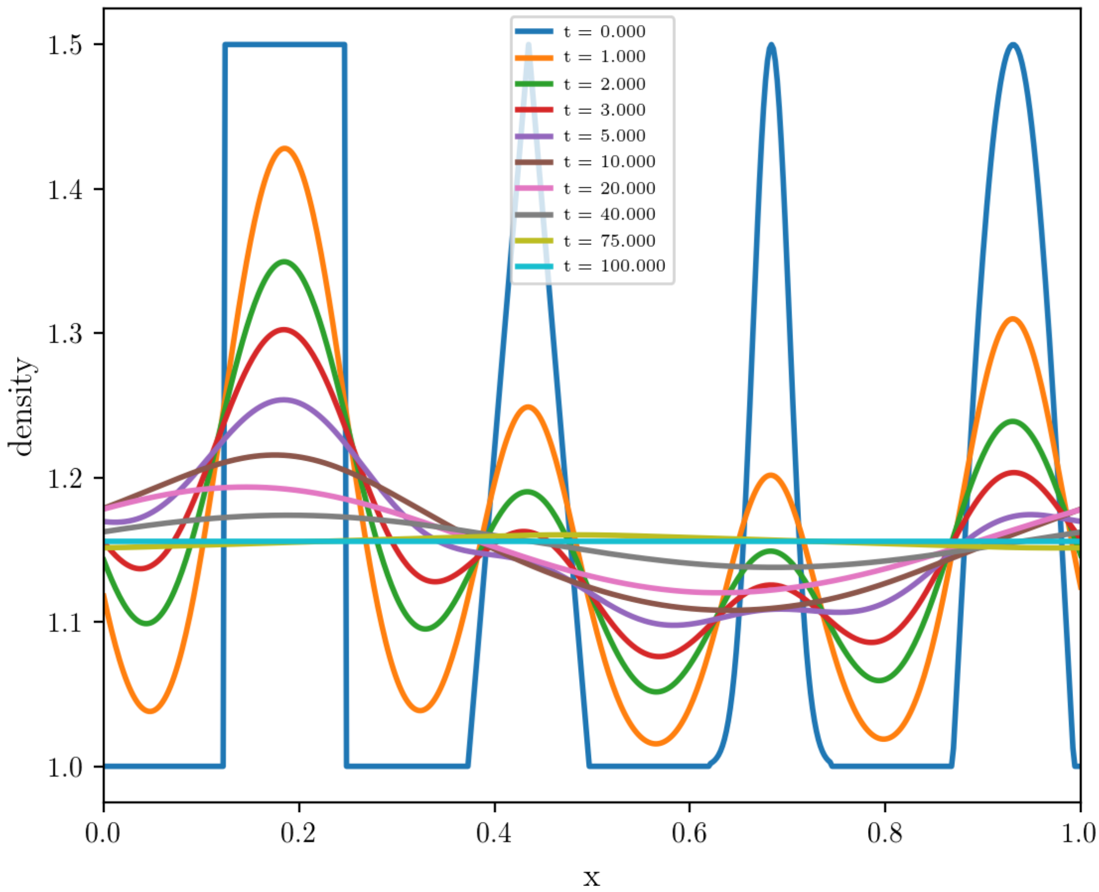

Figure 2: Piecewise constant advection with positive fixed global velocity $v_x = 1$. $C_{CFL} = 0.1$, $nx = 500$

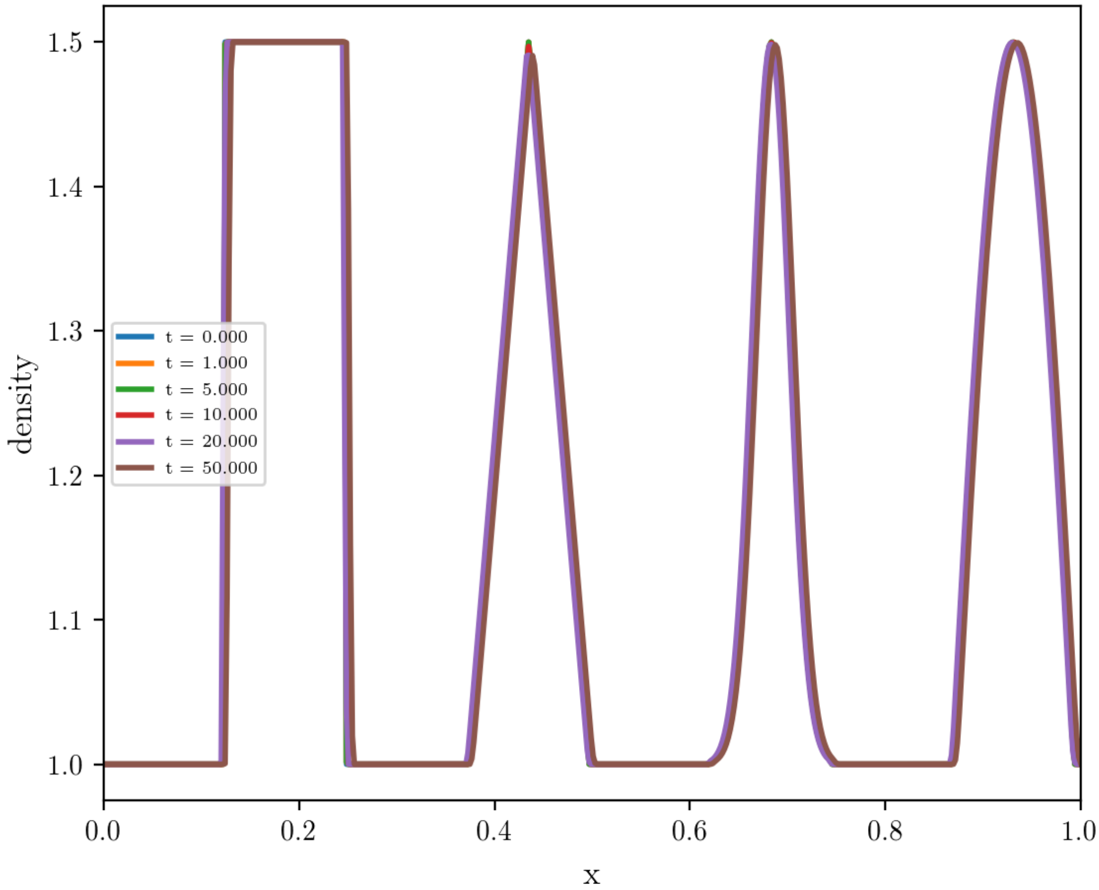

Figure 3: Piecewise constant advection with positive fixed global velocity $v_x = 1$. $C_{CFL} = 1.0$, $nx = 500$

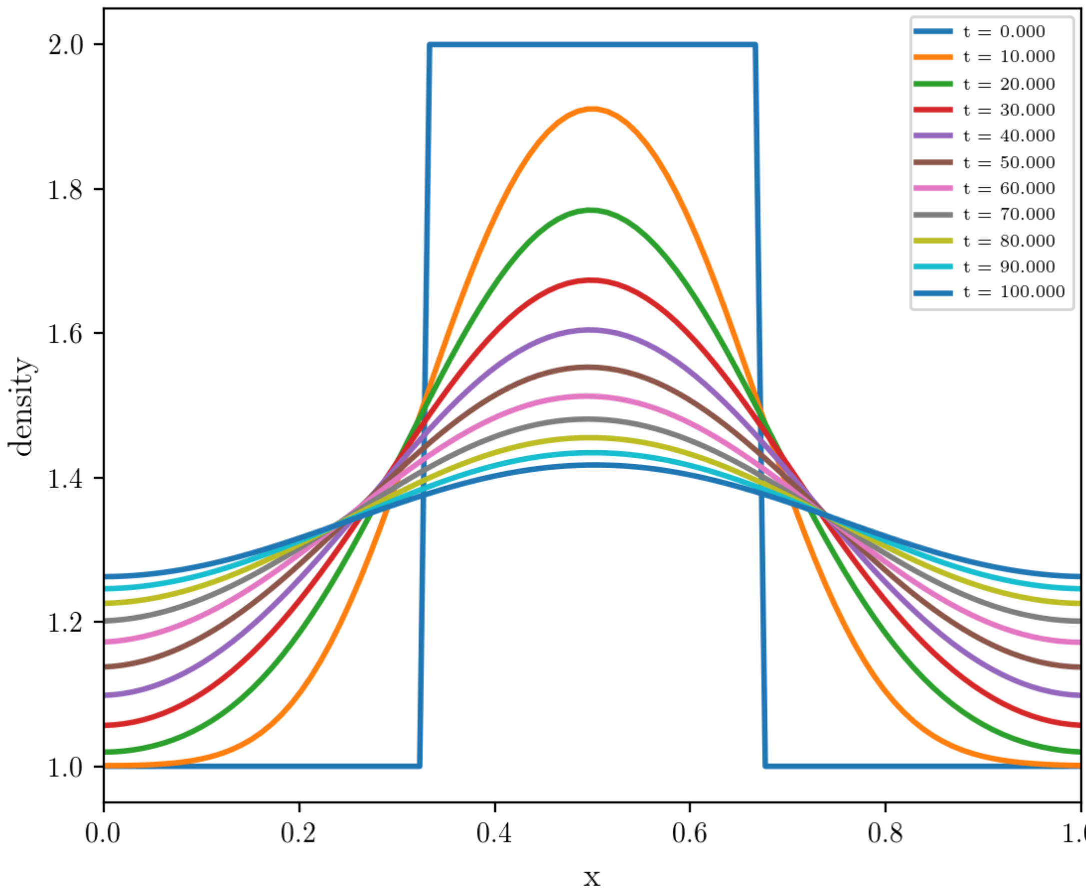

Figure 4: Piecewise constant advection with NEGATIVE fixed global velocity $v_x = -1$. $C_{CFL} = 0.9$, $nx = 100$

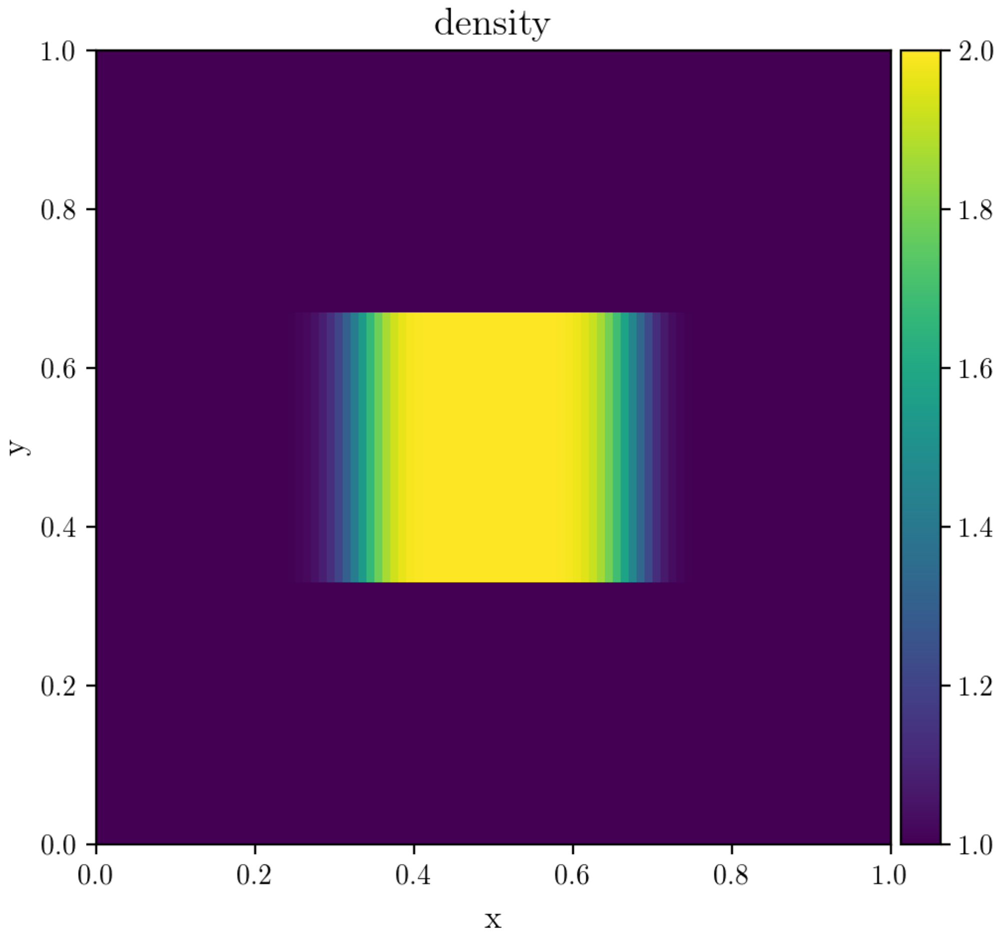

Figure 5: Piecewise constant advection with fixed global velocity $v_x = 1, v_y = 0$. $C_{CFL} = 0.9$, $nx = 100$. ICs were a step function. This is 2D **without** Strang splitting, done naively.

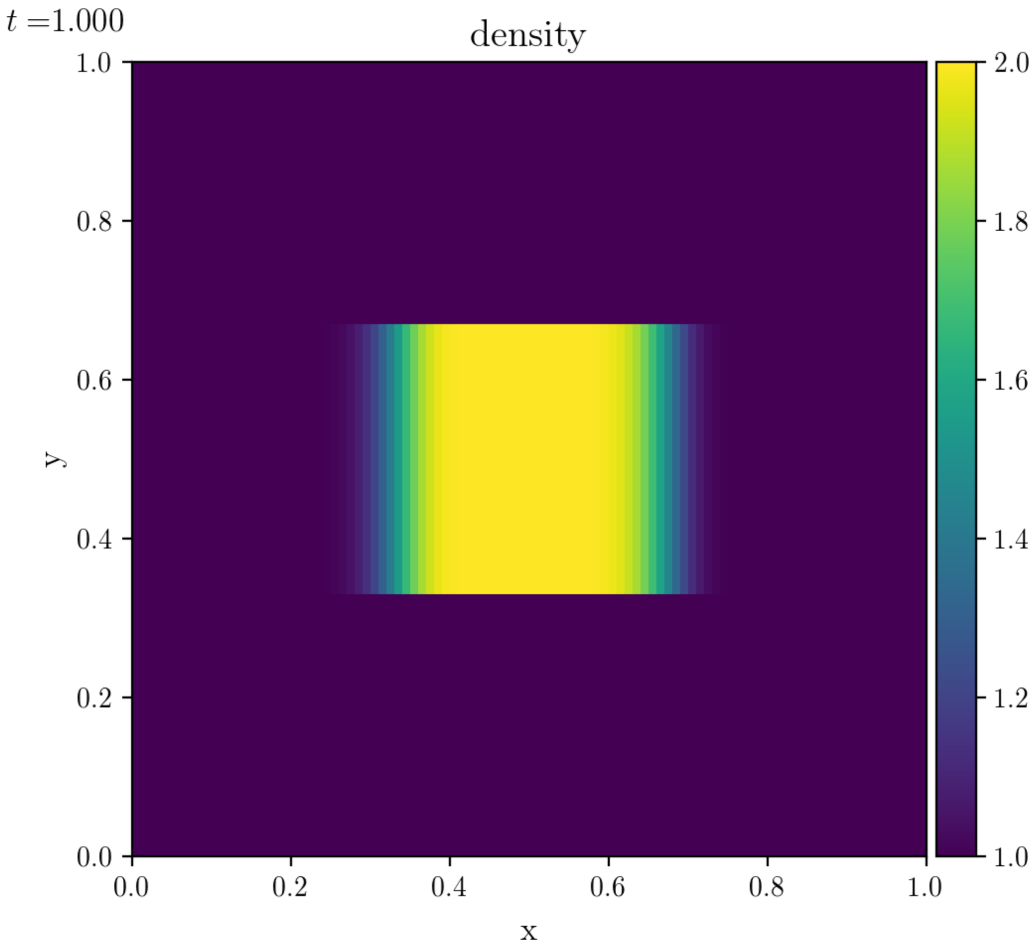

Figure 6: Piecewise constant advection with fixed global velocity $v_x = 1, v_y = 0$. $C_{CFL} = 0.9$, $nx = 100$. ICs were a step function. **With** Strang splitting.

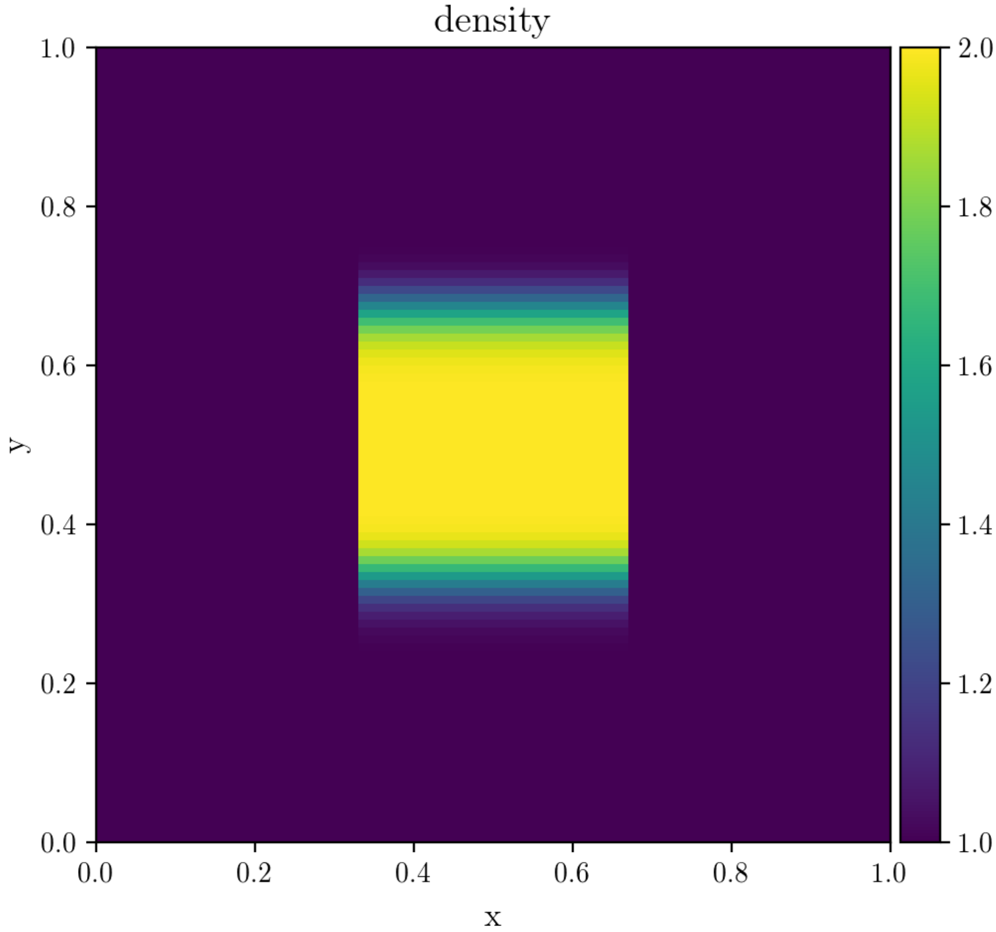

Figure 7: Piecewise constant advection with fixed global velocity $v_x = 0, v_y = 1$. $C_{CFL} = 0.9$, $nx = 100$, $t = 1$. ICs were a step function. **Without** Strang splitting, done naively.

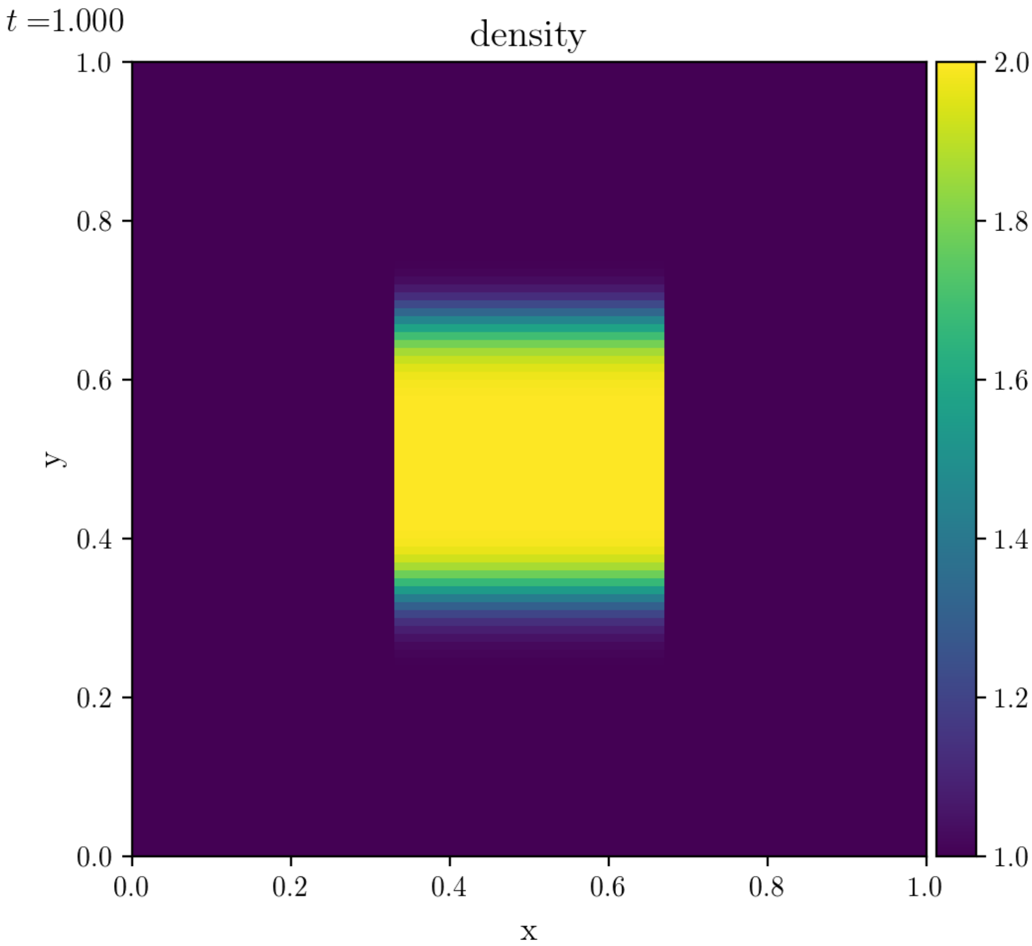

Figure 8: Piecewise constant advection with fixed global velocity $v_x = 0, v_y = 1$. $C_{CFL} = 0.9$, $nx = 100$, $t = 1$. ICs were a step function. **With** Strang splitting.

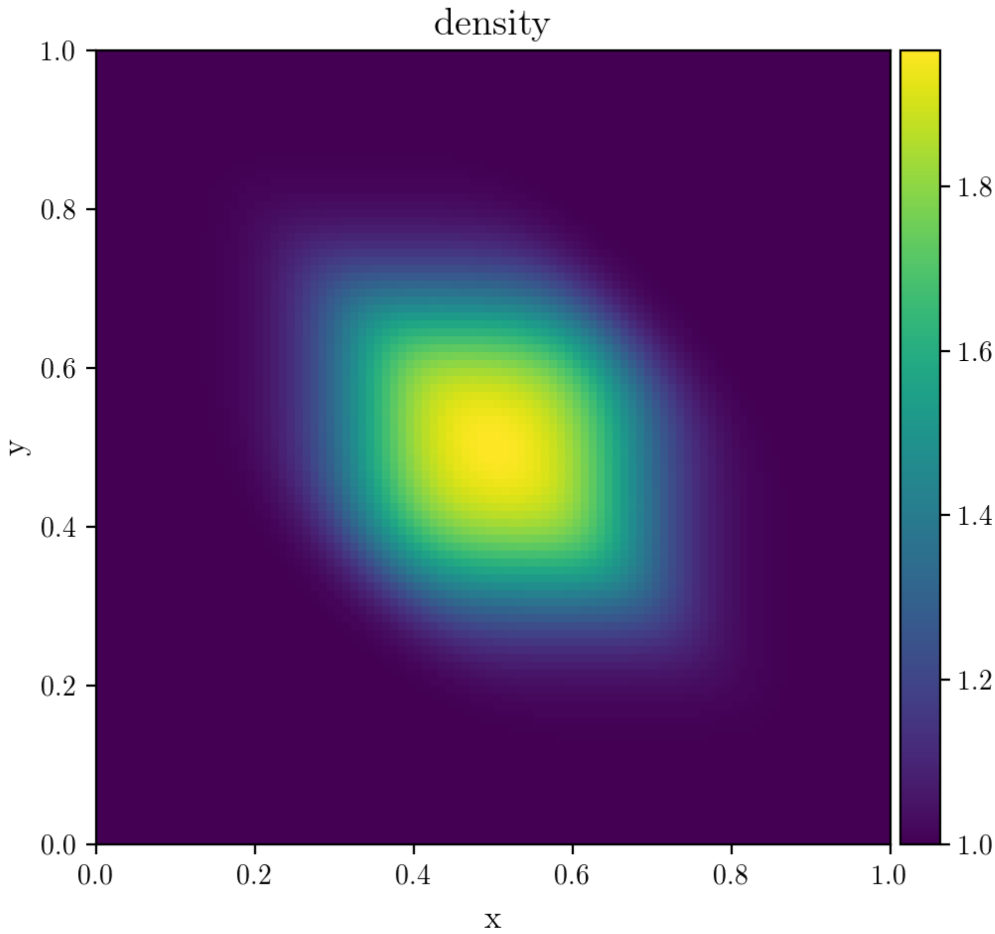

Figure 9: Piecewise constant advection with fixed global velocity $v_x = v_y = 1$. $C_{CFL} = 0.9$, $nx = 100$, $t = 1$. ICs were a step function. This is 2D **without** Strang splitting, done naively.

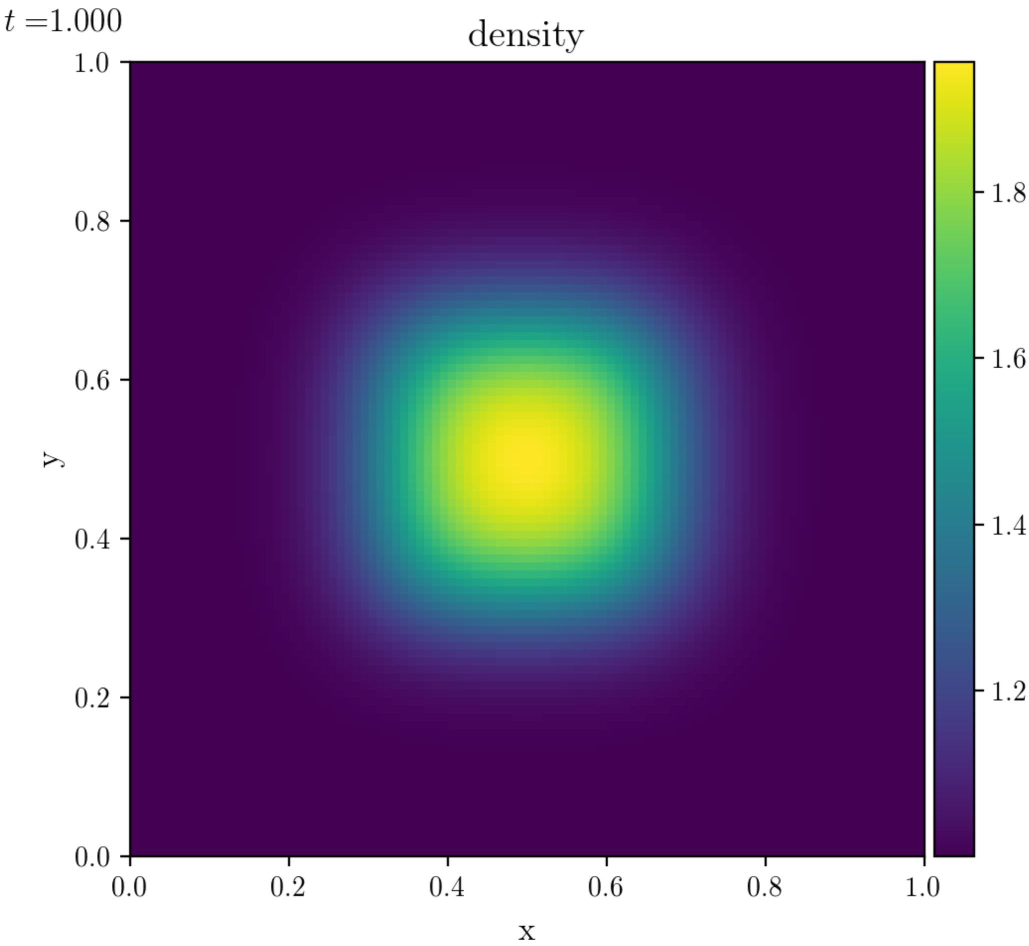

Figure 10: Piecewise constant advection with fixed global velocity $v_x = v_y = 1$. $C_{CFL} = 0.9$, $nx = 100$, $t = 1$. ICs were a step function. This is 2D **with** Strang splitting.

2.2 Piecewise Linear

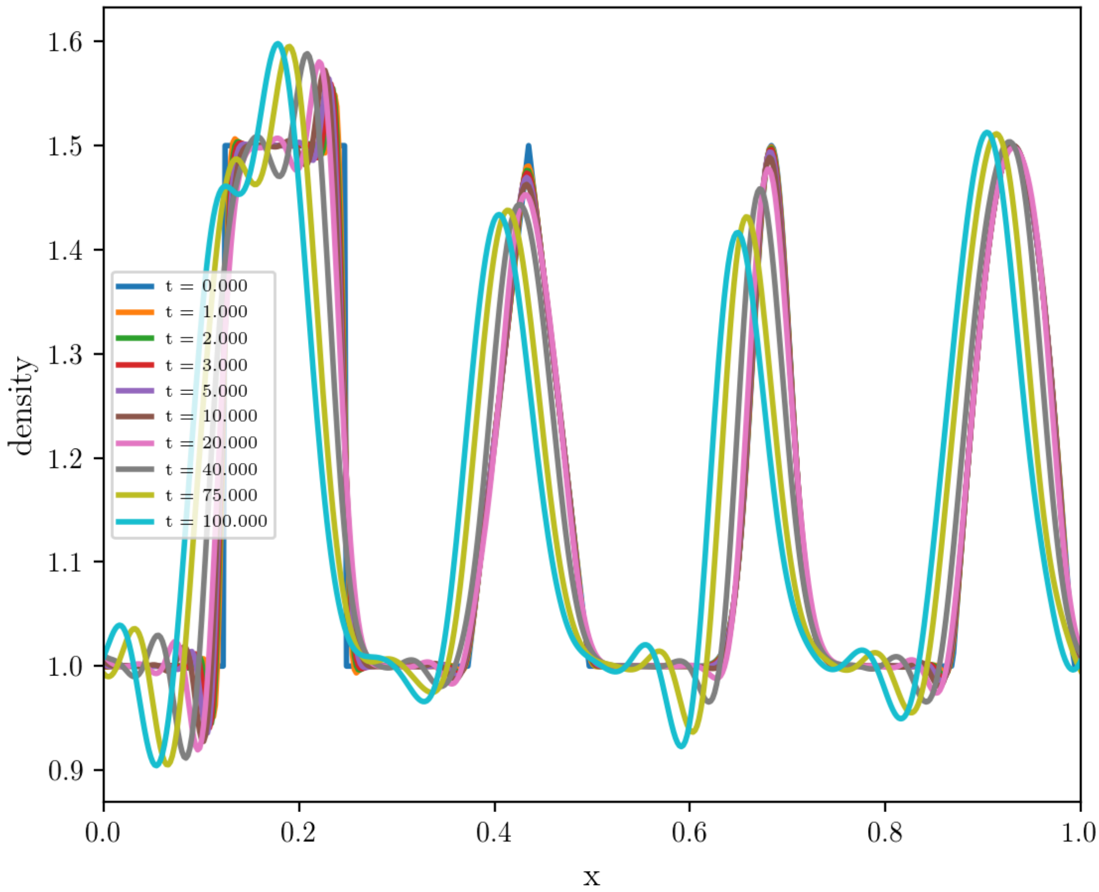

Figure 11: Piecewise linear advection with positive fixed global velocity $v_x = 1$. $C_{CFL} = 0.9$, $nx = 100$

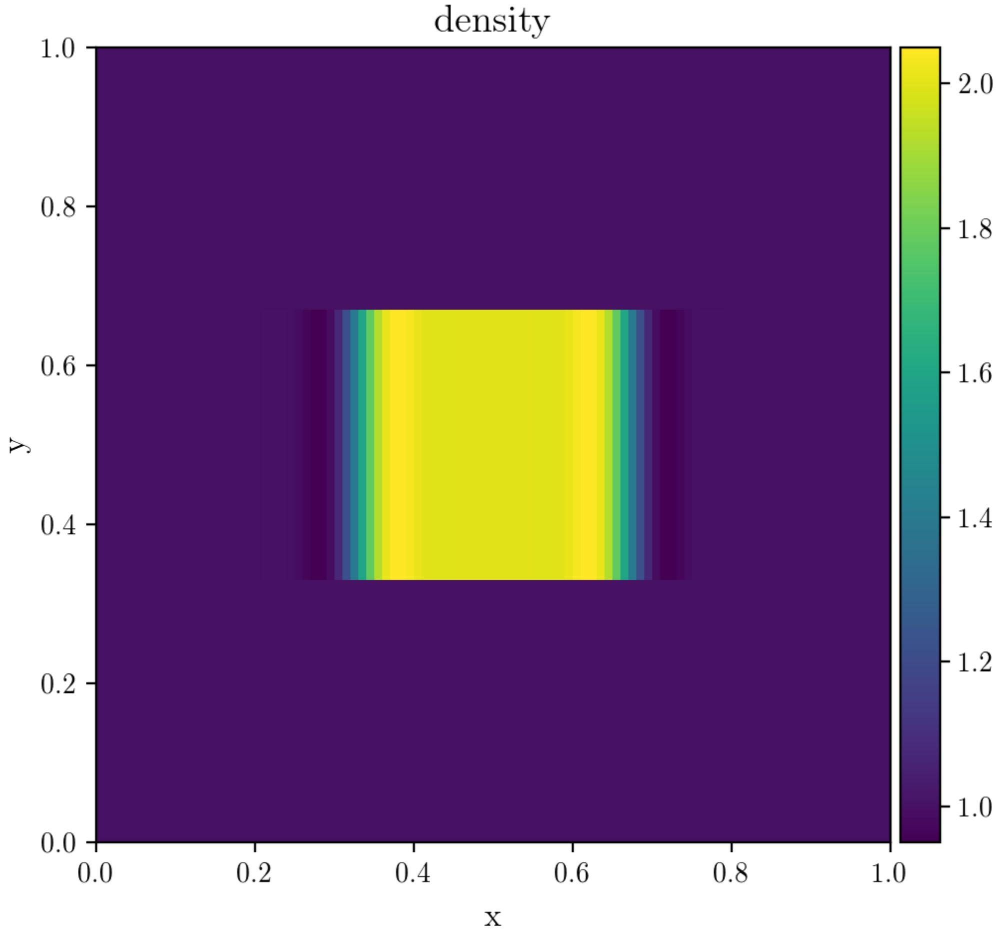

Figure 12: Piecewise linear advection with fixed global velocity $v_x = 1, v_y = 0$. $C_{CFL} = 0.9$, $nx = 100$. ICs were a step function. **Without** Strang splitting.

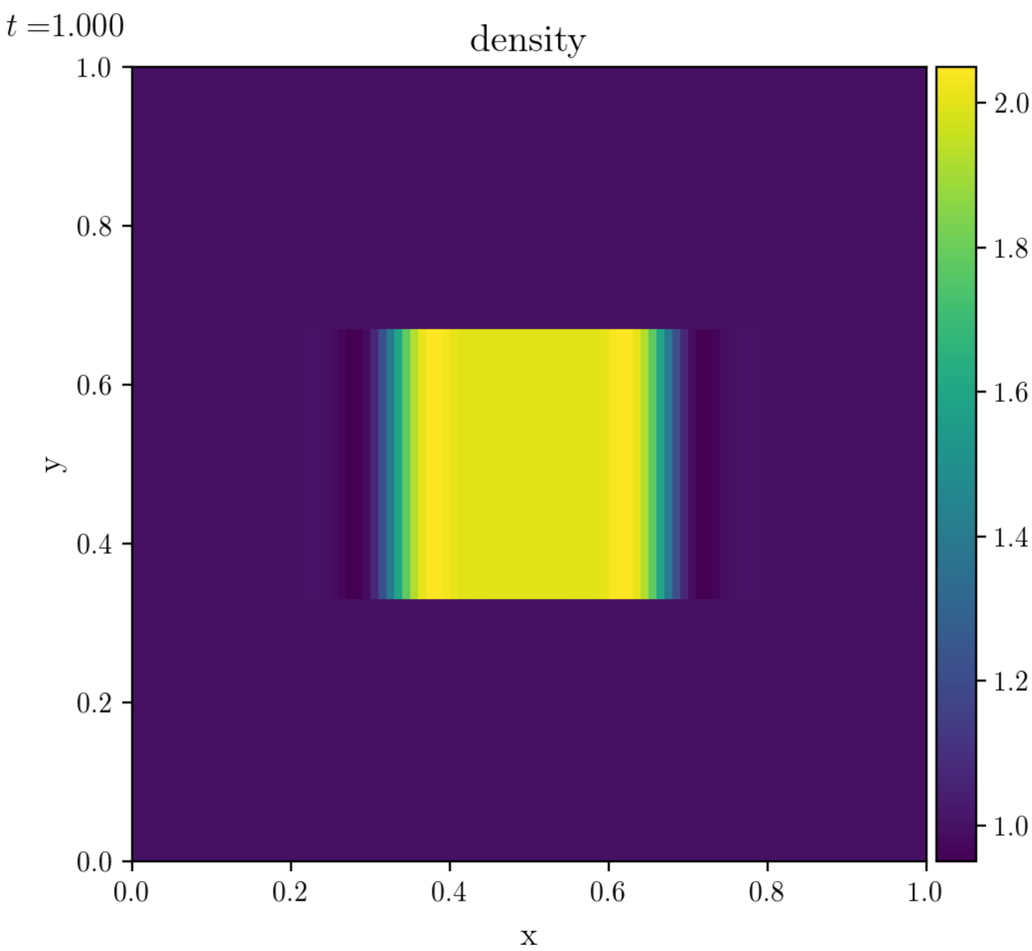

Figure 13: Piecewise linear advection with fixed global velocity $v_x = 1, v_y = 0$. $C_{CFL} = 0.9$, $nx = 100$. ICs were a step function. **With** Strang splitting.

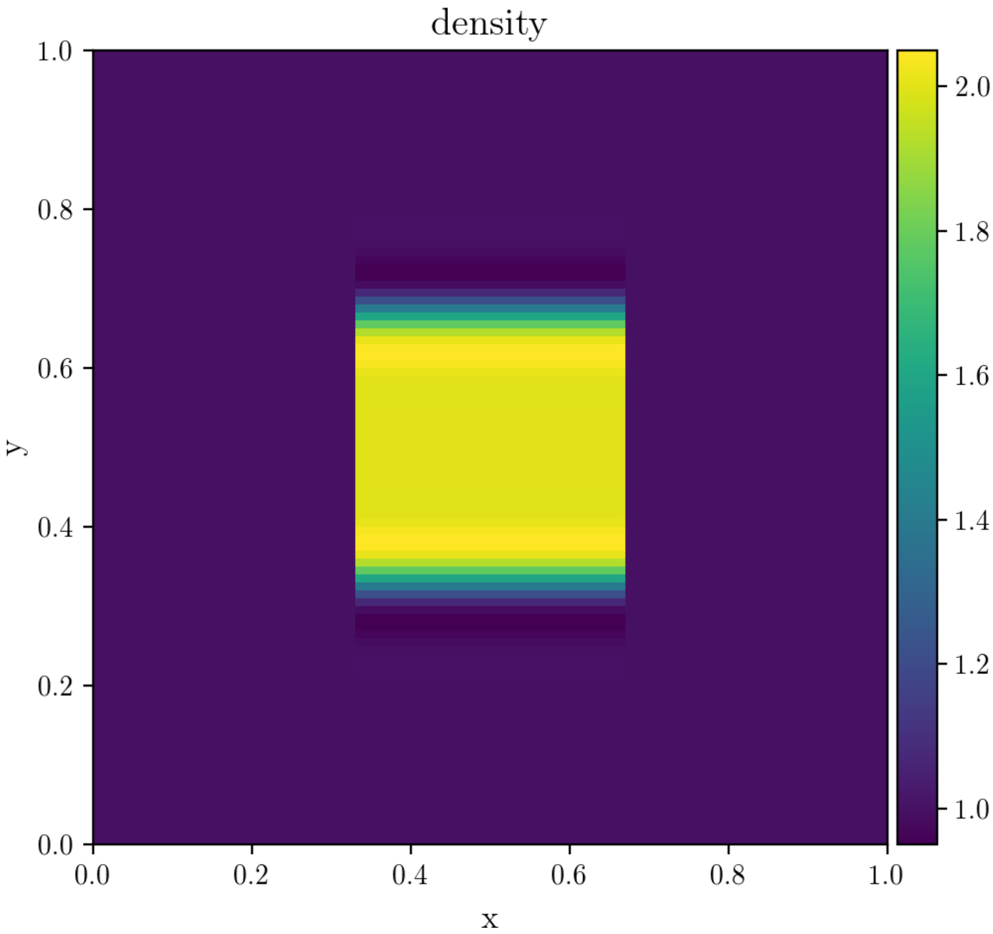

Figure 14: Piecewise linear advection with fixed global velocity $v_x = 0, v_y = 1$. $C_{CFL} = 0.9$, $nx = 100$. ICs were a step function. **Without** Strang splitting.

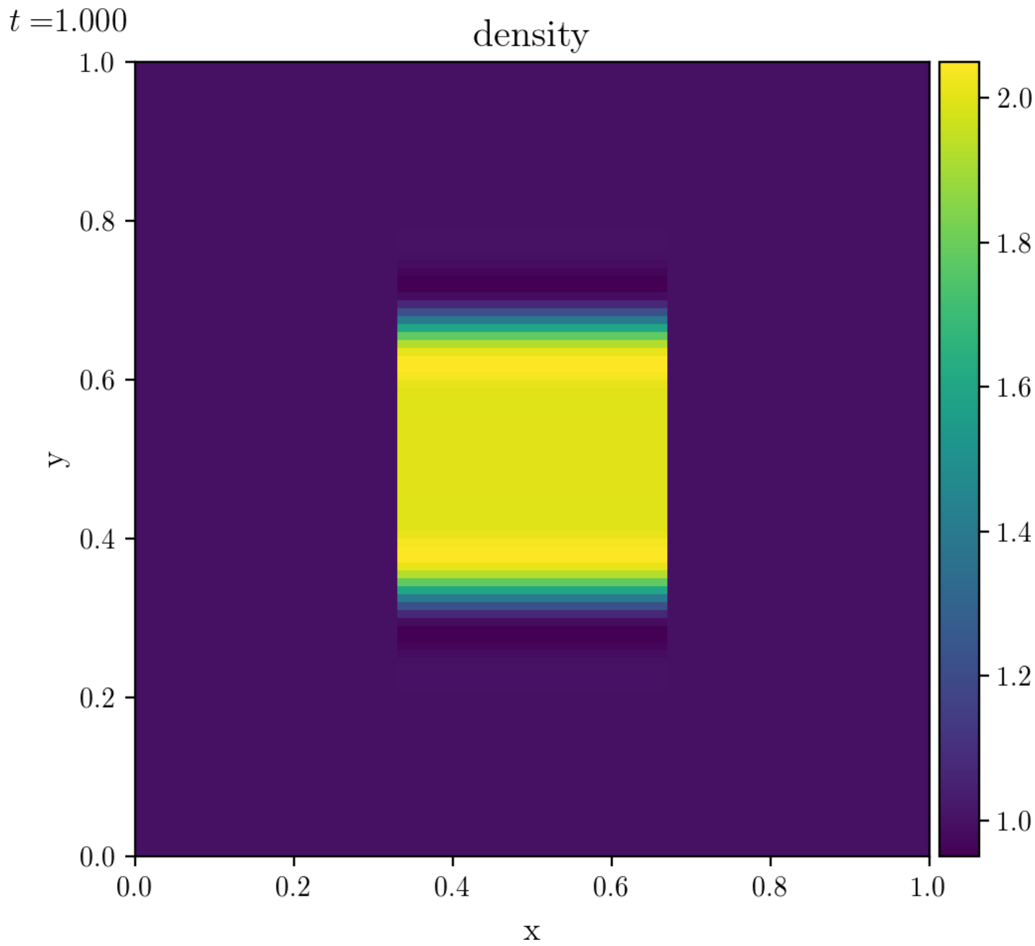

Figure 15: Piecewise linear advection with fixed global velocity $v_x = 0, v_y = 1$. $C_{CFL} = 0.9$, $nx = 100$. ICs were a step function. **With** Strang splitting.

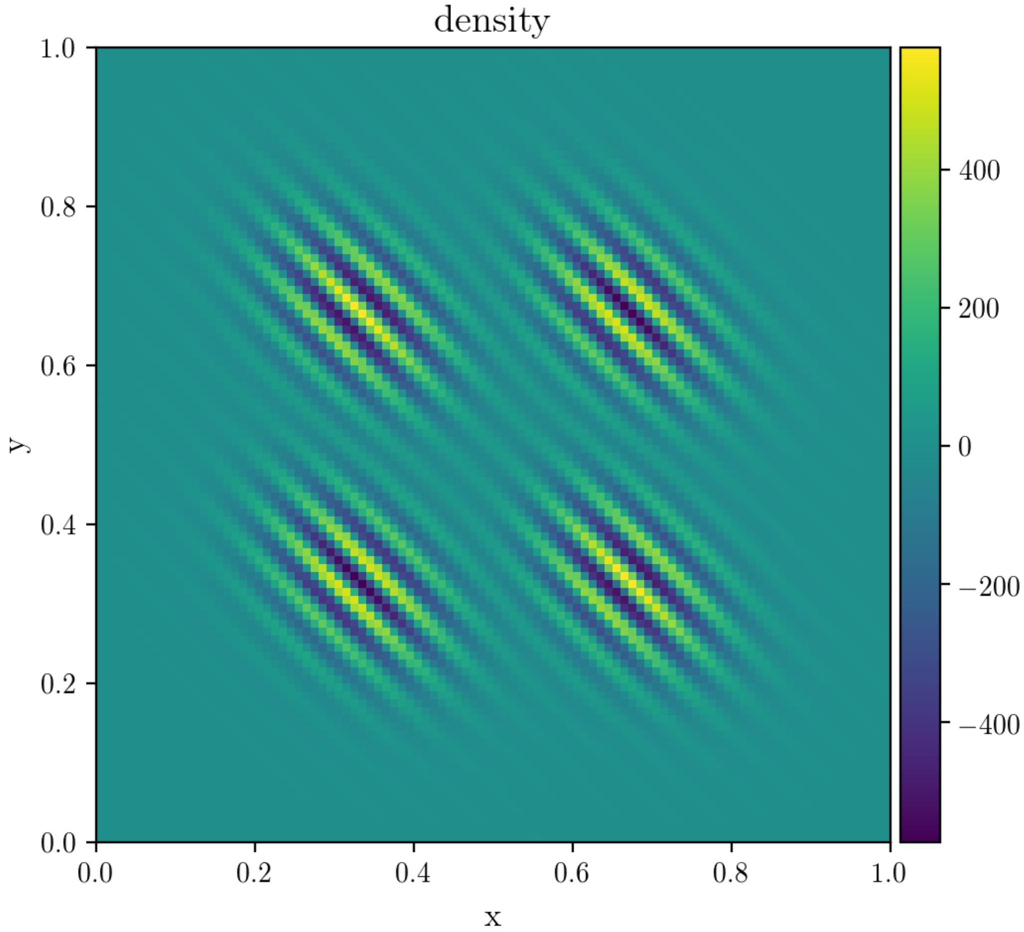

Figure 16: Piecewise linear advection with fixed global velocity $v_x = v_y = 1$. $C_{CFL} = 0.9$, $nx = 100$. ICs were a step function. Note that despite of the strong oscillations, the total density is conserved! (Unless the oscillations get too big for floats to handle). **Without** Strang splitting.

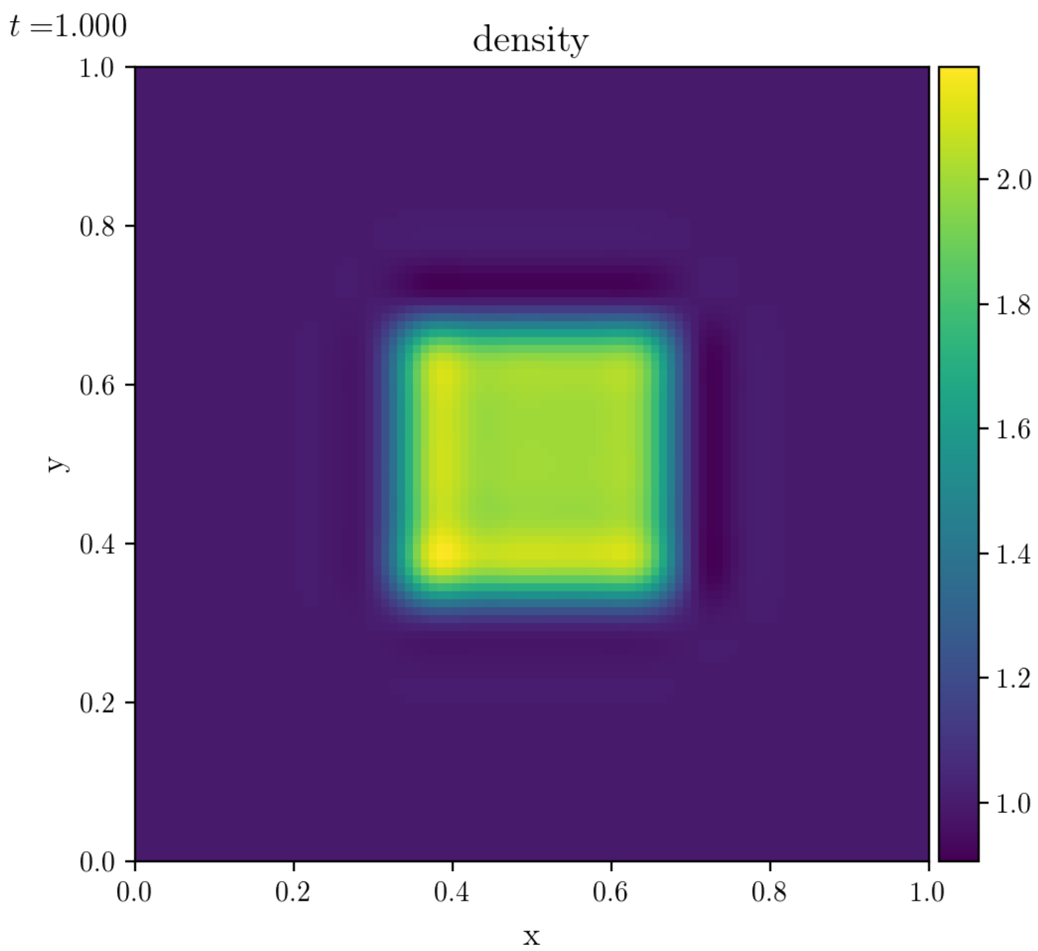

Figure 17: Piecewise linear advection with fixed global velocity $v_x = v_y = 1$. $C_{CFL} = 0.9$, $nx = 100$. ICs were a step function. Note that despite of the strong oscillations, the total density is conserved! (Unless the oscillations get too big for floats to handle) **With** Strang splitting.

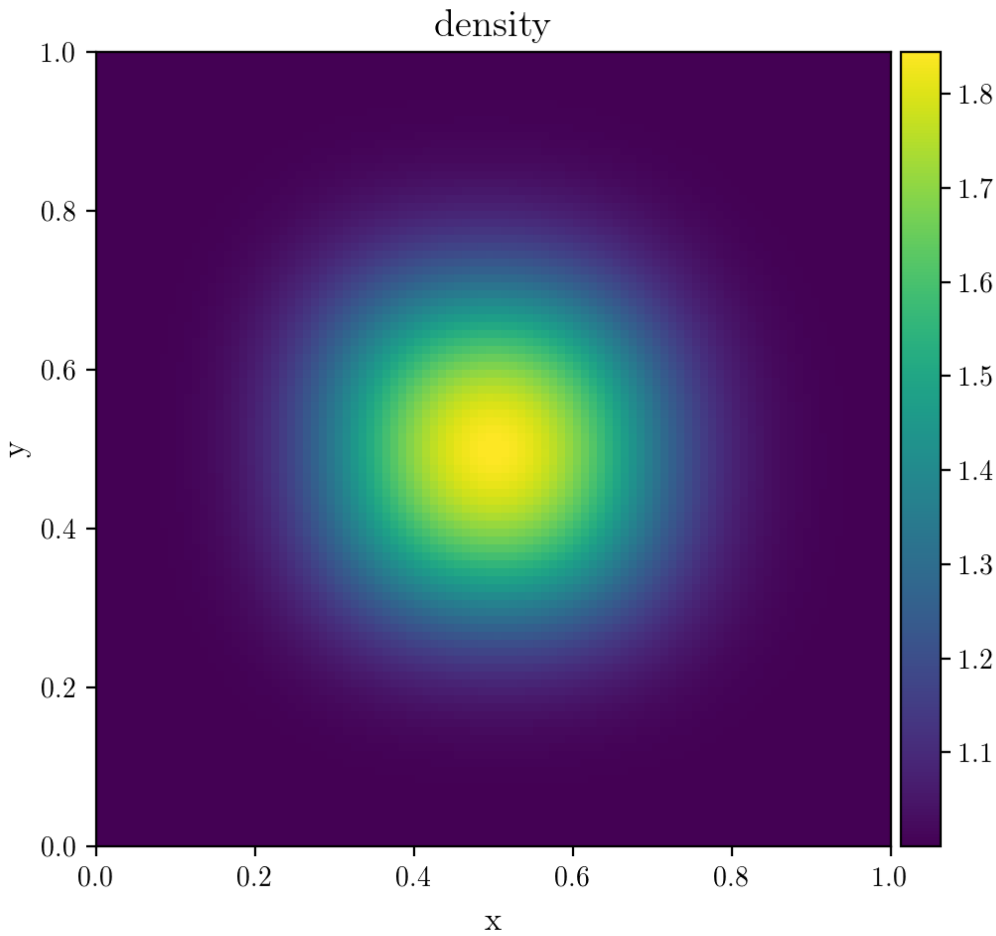

Figure 18: Piecewise linear advection with fixed global velocity $v_x = v_y = 1$. $C_{CFL} = 0.1$, $nx = 100$. ICs were a step function. Note the lower CFL condition compared to fig 16. **Without** Strang splitting.

2.3 Order of Convergence

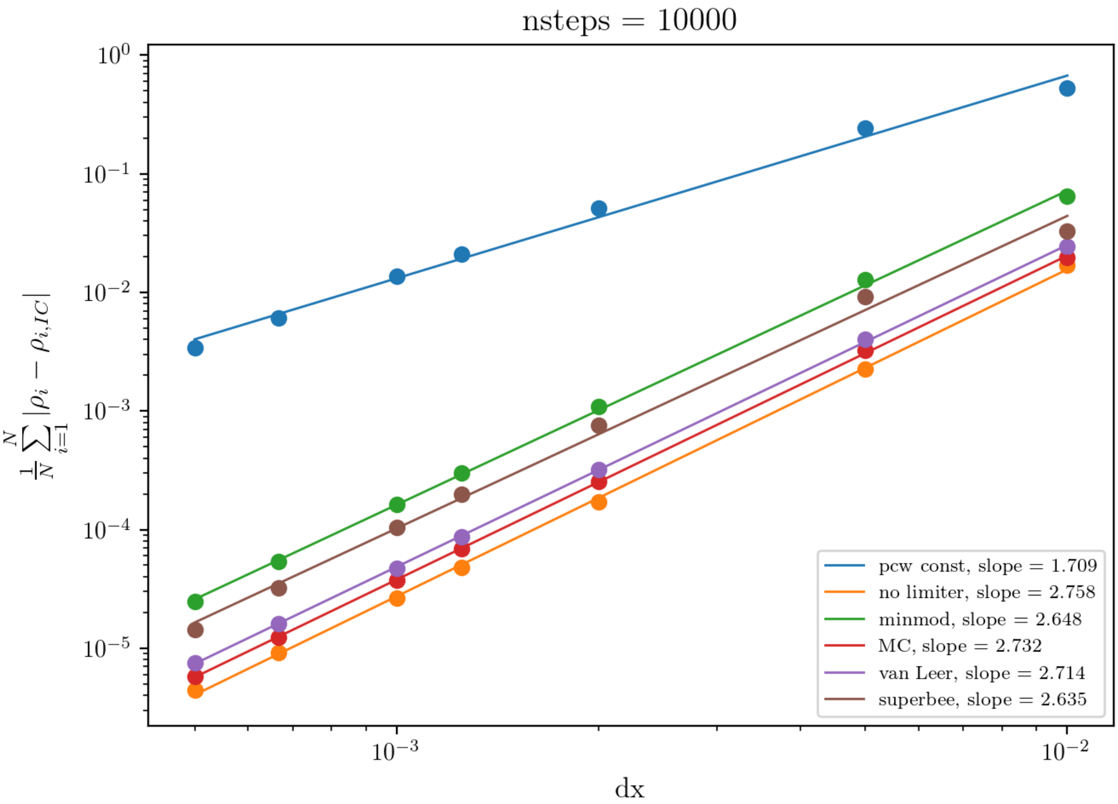

Figure 19: Convergence Study with respect to cell size Δx using the $L1$ norm. Points are measurements, the straight lines are fitted curves, with their slope given in the legend. For an accurate comparison, the simulations are stopped after the same number of steps. This way, the C_{cfl} can also be kept constant throughout the different Δx. Initial conditions was a Gaussian profile.

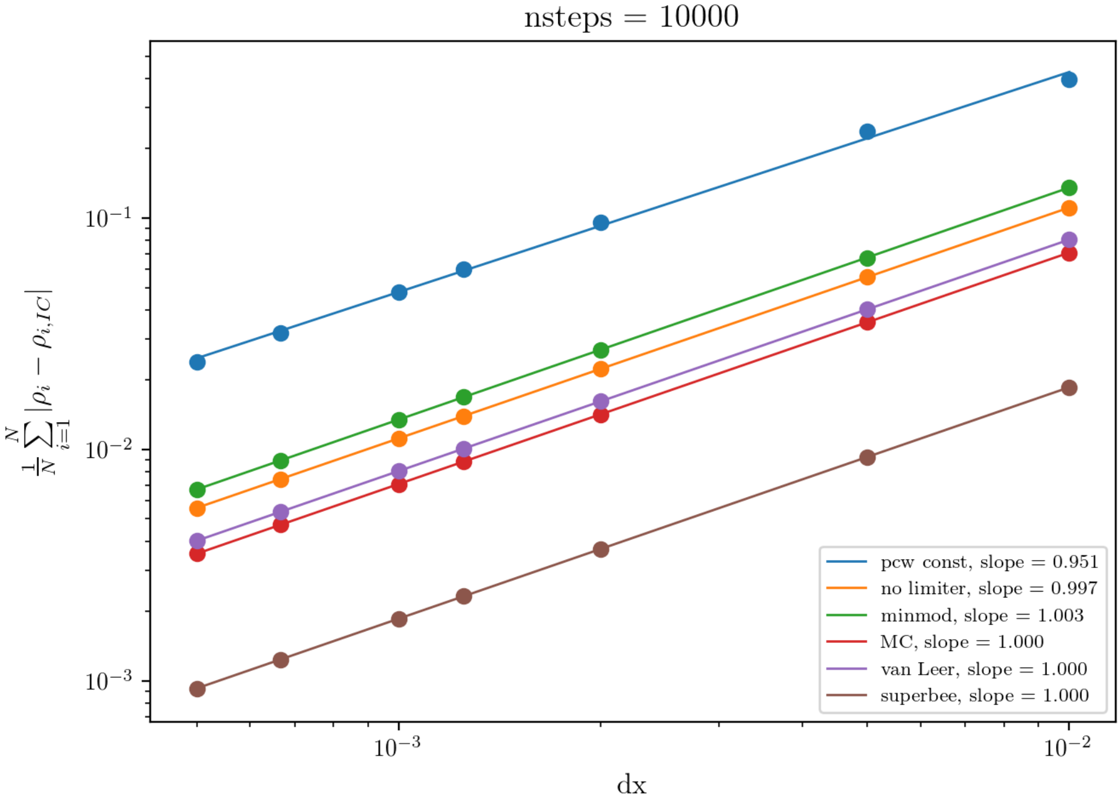

Figure 20: Convergence Study with respect to cell size Δx using the $L1$ norm. Points are measurements, the straight lines are fitted curves, with their slope given in the legend. For an accurate comparison, the simulations are stopped after the same number of steps. This way, the C_{cfl} can also be kept constant throughout the different Δx. Initial conditions was a step function.

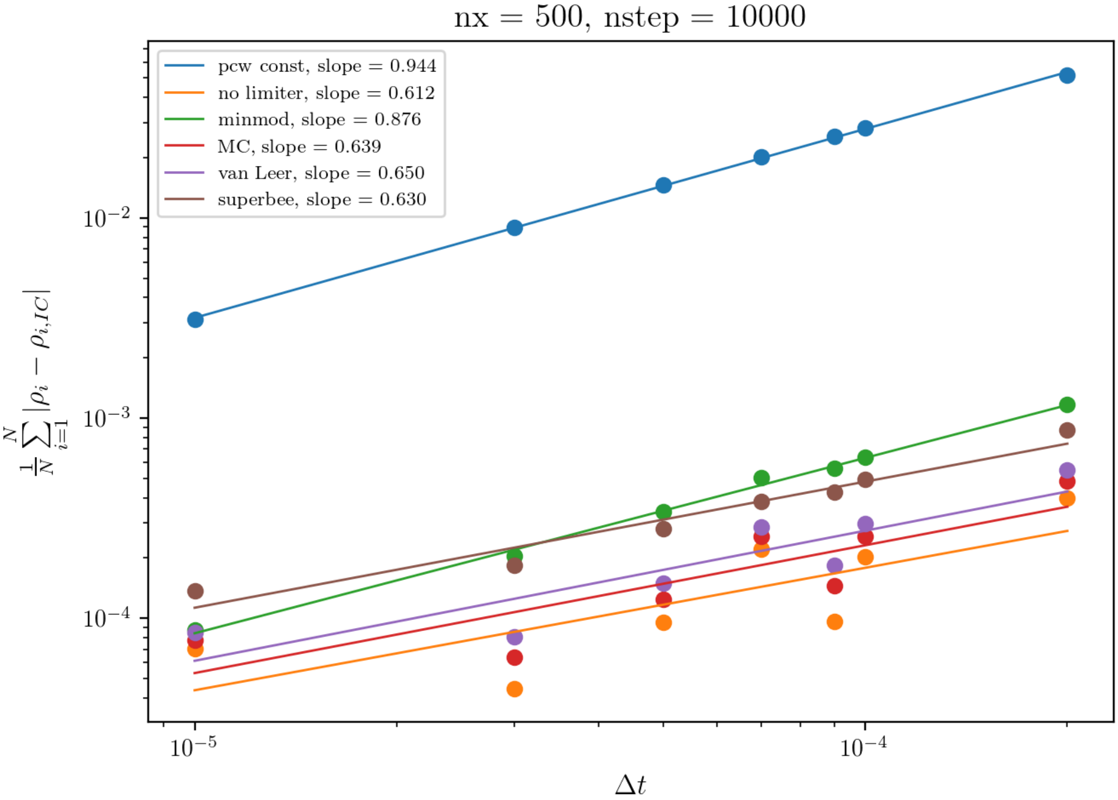

Figure 21: Convergence Study with respect to time step size Δt using the $L1$ norm. Points are measurements, the straight lines are fitted curves, with their slope given in the legend. For an accurate comparison, the simulations are stopped after the same number of steps, and Δx is kept constant. Highest Δt corresponds to $C_{cfl} = 0.001$. Initial conditions was a Gaussian profile.

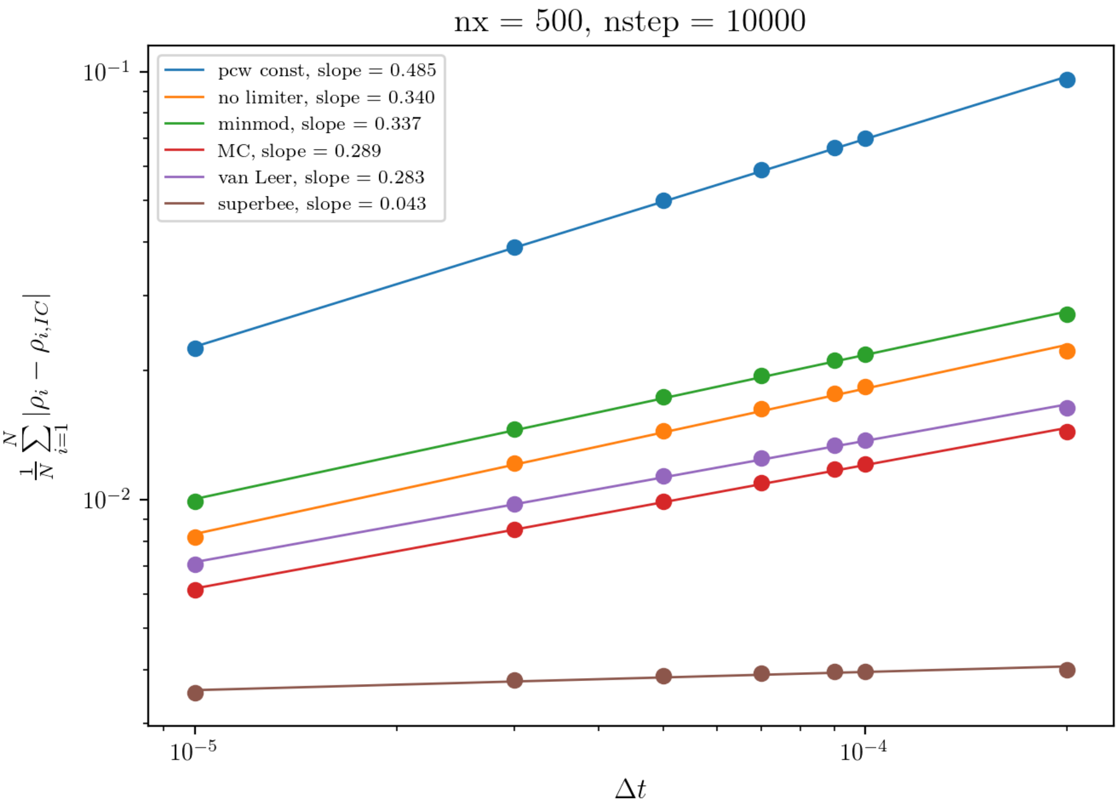

Figure 22: Convergence Study with respect to time step size Δt using the $L1$ norm. Points are measurements, the straight lines are fitted curves, with their slope given in the legend. For an accurate comparison, the simulations are stopped after the same number of steps, and Δx is kept constant. Highest Δt corresponds to $C_{cfl} = 0.001$. Initial conditions was a step function.

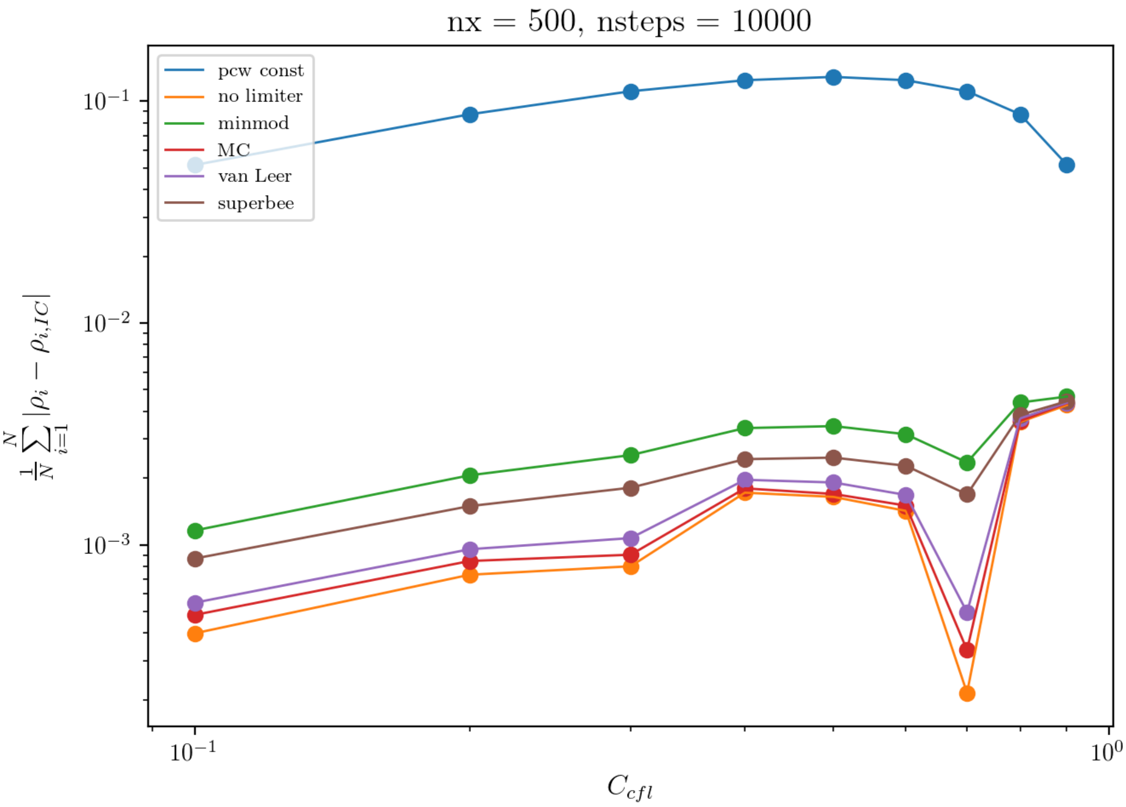

Figure 23: Convergence Study with respect to the Courant number C_{cfl} using the $L1$ norm. Points are measurements, the straight lines just connect the dots. For an accurate comparison, the simulations are stopped after the same number of steps, and Δx is kept constant. Initial conditions was a Gaussian profile.

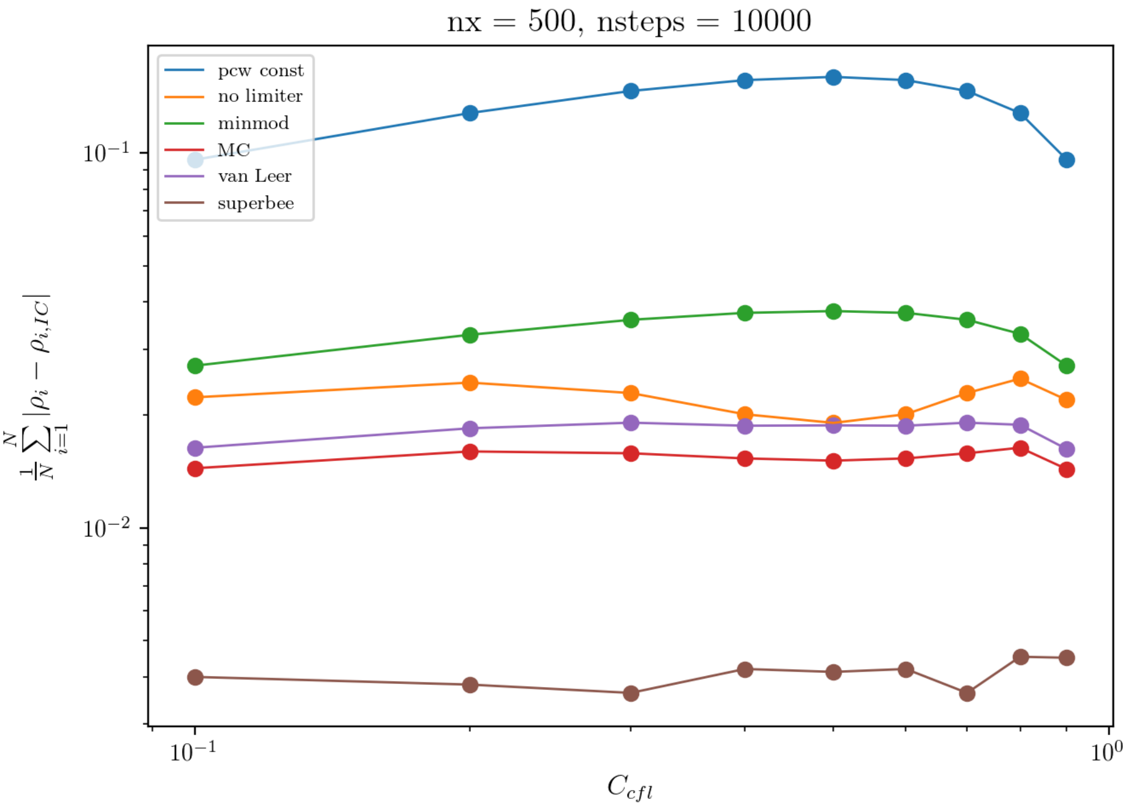

Figure 24: Convergence Study with respect to the Courant number C_{cfl} using the $L1$ norm. Points are measurements, the straight lines just connect the dots. For an accurate comparison, the simulations are stopped after the same number of steps, and Δx is kept constant. Initial conditions was a step function.

2.4 Conclusions

- Advection is diffusive (fig 1).
- It is diffusive even if $C_{CFL} = 1$! (fig 3). This is most probably because of round-off/float errors. For high t, the whole shape moves a bit to the right even.
- Using a lower CFL number leads to stronger diffusion. Compare figs. 1 and 2. Why?

  We are solving the 1D advection equation with c being a constant velocity:

$$\frac{\partial u}{\partial t} + c\frac{\partial u}{\partial x} = 0 \tag{1}$$

Discretising this equation, we get (using an explicit time scheme and upwind differencing):

$$\frac{u_i^{n+1} - u_i^n}{\Delta t} + \frac{u_i^n - u_{i-1}^n}{\Delta x} = 0 \tag{2}$$

This is however not an exact expression, but only an approximate one. If we use a Taylor expansion

$$u_i^{n+1} = u_i^n + \Delta t \frac{\partial u}{\partial t} + \frac{\Delta t^2}{2}\frac{\partial^2 u}{\partial t^2} + O(\Delta t^3) \tag{3}$$
$$u_{i-1}^n = u_i^n - \Delta x \frac{\partial u}{\partial x} + \frac{\Delta x^2}{2}\frac{\partial^2 u}{\partial x^2} + O(\Delta x^3) \tag{4}$$

and insert it into eq 2, we get (neglecting third order terms from now on)

$$\frac{\partial u}{\partial t} + c\frac{\partial u}{\partial x} + \frac{1}{2}\Delta t \frac{\partial^2 u}{\partial t^2} - c\frac{\Delta x}{2}\frac{\partial^2 u}{\partial x^2} = 0 \tag{5}$$

$$\Rightarrow \frac{\partial u}{\partial t} + c\frac{\partial u}{\partial x} = -\frac{1}{2}\Delta t \frac{\partial^2 u}{\partial t^2} + c\frac{\Delta x}{2}\frac{\partial^2 u}{\partial x^2} \tag{6}$$
$$= 0 + Err \tag{7}$$
$$Err = -\frac{1}{2}\Delta t \frac{\partial^2 u}{\partial t^2} + c\frac{\Delta x}{2}\frac{\partial^2 u}{\partial x^2} \tag{8}$$

which is the advection equation 1 plus some error term.

Now using eq. 1 we find:

$$\frac{\partial u}{\partial t} + c\frac{\partial u}{\partial x} = 0 \tag{9}$$
$$1) \quad \frac{\partial^2 u}{\partial t2} + c\frac{\partial^2 u}{\partial t \partial x} = 0 \tag{10}$$
$$2) \quad \frac{\partial u}{\partial t} = -c\frac{\partial u}{\partial x} \tag{11}$$
$$\Rightarrow \quad 3) \quad \frac{\partial^2 u}{\partial t^2} - c^2\frac{\partial^2 u}{\partial x^2} = 0 \tag{12}$$

This gives us for the error term:

$$
\begin{aligned}
Err &= -\frac{1}{2}\Delta t \frac{\partial^2 u}{\partial t^2} + c\frac{\Delta x}{2}\frac{\partial^2 u}{\partial x^2} && (13)\\
&= -\frac{c^2 \Delta t}{2}\frac{\partial^2 u}{\partial x^2} + c\frac{\Delta x}{2}\frac{\partial^2 u}{\partial x^2} && (14)\\
&= \frac{c\Delta x}{2}\left(1 - \frac{c\Delta t}{\Delta x}\right)\frac{\partial^2 u}{\partial x^2} && (15)
\end{aligned}
$$

Inserting the CFL condition:

$$
\frac{c\Delta t_{max}}{\Delta x} = C_{cfl} \leq 1 \tag{16}
$$

we obtain:

$$
Err = \frac{c\Delta x}{2}\left(1 - C_{cfl}\right)\frac{\partial^2 u}{\partial x^2} \tag{17}
$$

The second derivative in space is characteristic for diffusion. But you can immediately see that the diffusion term (coefficient) depends on C_{cfl}, and indeed increases with decreasing C_{cfl}!

- 2D advection:

  For advection only in x or y direction, respectively, the method reduces to the one dimensional case, and the results are identical when using Strang splitting or the naive case. Compare figs 5 vs 6, and 7 vs 8. But when we have both v_x and v_y be non-zero, the naive method (i.e. without Strang splitting, where we just extend the 1D method to 2D and don't think about it) starts getting "stripes" perpendicular to the diagonal along which it is being advected along (fig 9 vs 10). The reason is that a) the upwinding is not complete, i.e. the value $u_{i-1,j-1}$ along the diagonal in the naive case never gets properly advected to $u_{i,j}$, and b) the method is diffusive, so the diffused material from $u_{i-1,j}$ and $u_{i,j-1}$ come together in that cell, messing everything up. Letting the code run for longer times actually leads to stripe-like instabilities. See also fig 16.

- The piecewise linear scheme can/will introduce oscillations around sharp edges (fig 11. The oscillations can go into the negative regime. Even though it's unphysical, the total density content remains constant! This is because the scheme is fundamentally conservative.

- On the order of convergence:

  - Dependence on Δx:

    For the smooth Gaussian profile IC: The results are nicely as expected, fig. 19. The piecewise constant advection is of $\mathcal{O}(\Delta x)$, piecewise linear is of $\mathcal{O}(\Delta x^2)$. Remember that the order of convergence computation on paper gives you only the upper boundary of the error, so a faster convergence is possible, but shouldn't be greater than 1 order than predicted, which we have here.

    For the step function in fig 20 we see as expected that the convergence rate drops to $\mathcal{O}(\Delta x)$ because that's what slope limiters do. So then why is the unlimited linear method also dropping to first order? The computations we did on paper for the order estimate assume a smooth initial condition, which we don't have here. It turns out having a discontinuity drops your order of convergence.

  - Dependence on Δt:

    Fixing the time step Δt is essentially the same as fixing the Courant number C_{cfl} for an already fixed velocity u and grid spacing Δx. For the order of convergence to be measured w.r.t. Δt, we must start with a Δt that implies a very low C_{cfl}. The reason is that C_{cfl} determines the amplitude of the diffusivity, see eqn. 17 and fig. 23 So for a good comparison, we need to start with a low enough C_{cfl} such that the difference in diffusivity is negligible. Otherwise, you don't see the power law that emerges.

    In the following analysis, let's focus on piecewise constant (first order) advection alone. I don't have the theory present for the piecewise linear scheme to back up my findings. What makes things more difficult is that for the piecewise linear advection, Δt also enters the computation of the fluxes between the cells, thus also affects the spatial component. It is not trivial to separate between the Δx and Δx dependence in these cases.

    For the Gaussian profile, fig. 21, we get a nice power law with slope 1, as expected. (The piecewise linear methods get close to $\mathcal{O}(\Delta t^{1/2})$. Maybe because they start developing jump discontinuities? Compare fig 37.) For the step profile of the piecewise constant advection, fig. 22, we get $\mathcal{O}(\Delta t^{1/2})$. The reason behind it is that the convergence analysis in theory assumes a smooth initial condition, such that we can use derivatives and Taylor-expansions.

The step function is not smooth though. It can be shown that for a jump discontinuity, the error goes as

$$Err \propto \sqrt{t}$$

So if we have N steps of equal size Δt), if we keep N constant, we get

$$Err \propto \sqrt{\Delta t} \tag{18}$$

See LeVeque 2002, chapter 8.6 for details.

which is exactly what we see in fig. 22.

– Dependence on C_{CFL}:

  Tweaking around C_{CFL} for a fixed nx and advection velocity u is essentially the same as tweaking Δt. For C_{cfl} comparable to 1 however we see the effects of the increased diffusivity, as described by equation 17. Indeed, measuring the convergence of $0.1 \leq C_{cfl} \leq 0.9$ in figs. 23 and 24 shows that it doesn't behave like a power law at all.

2.5 Future Debugging Hints

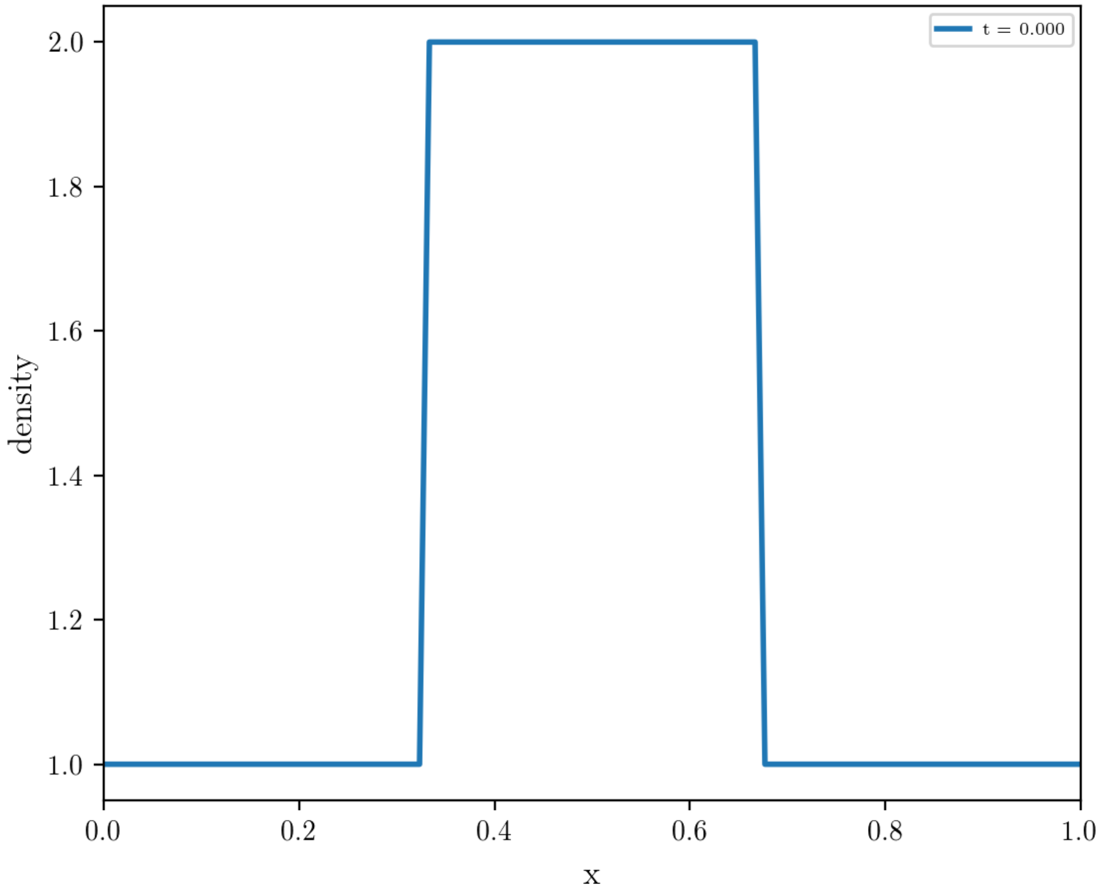

Figure 25: Initial conditions used to demonstrate debugging hints. $u = 1$.

2.5.1 When you're using downwind differencing

Downwind differencing is unphysical and violently unstable. Note how the wave goes in the wrong direction!

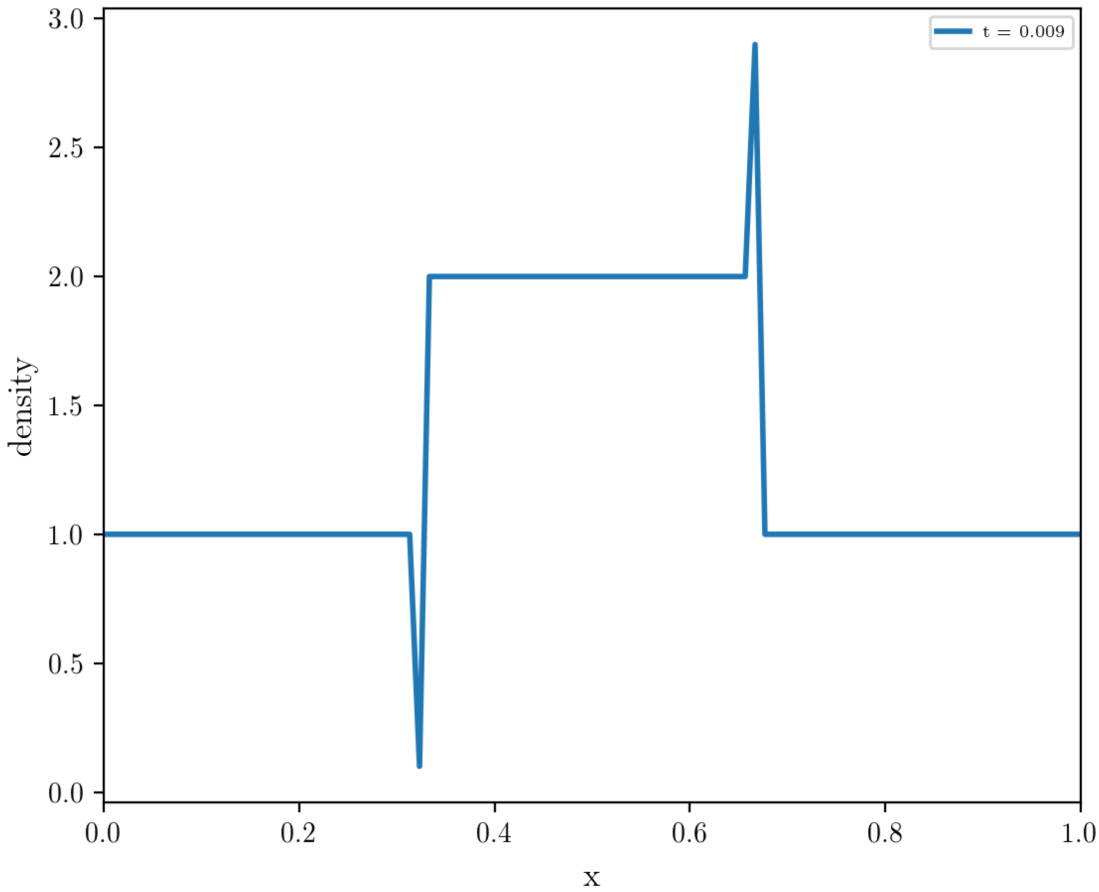

Figure 26: Downwind differencing after 1 step.

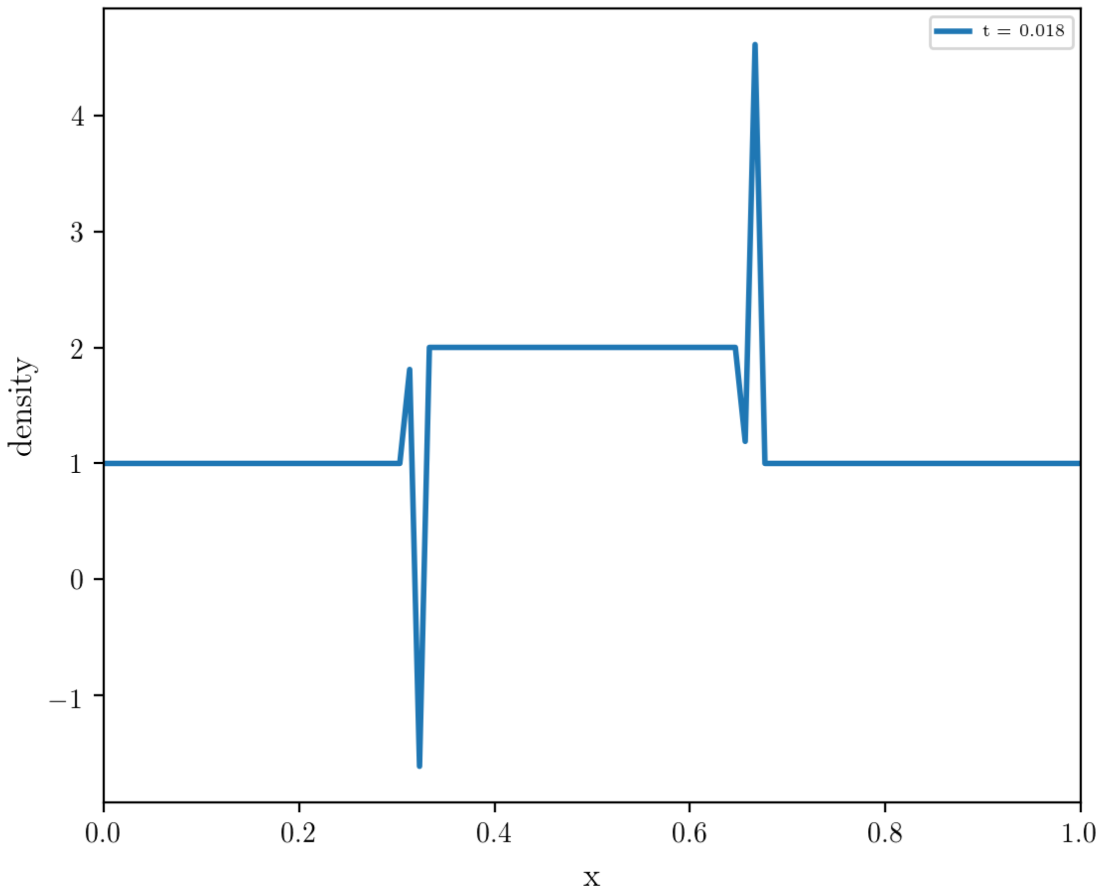

Figure 27: Downwind differencing after 2 steps.

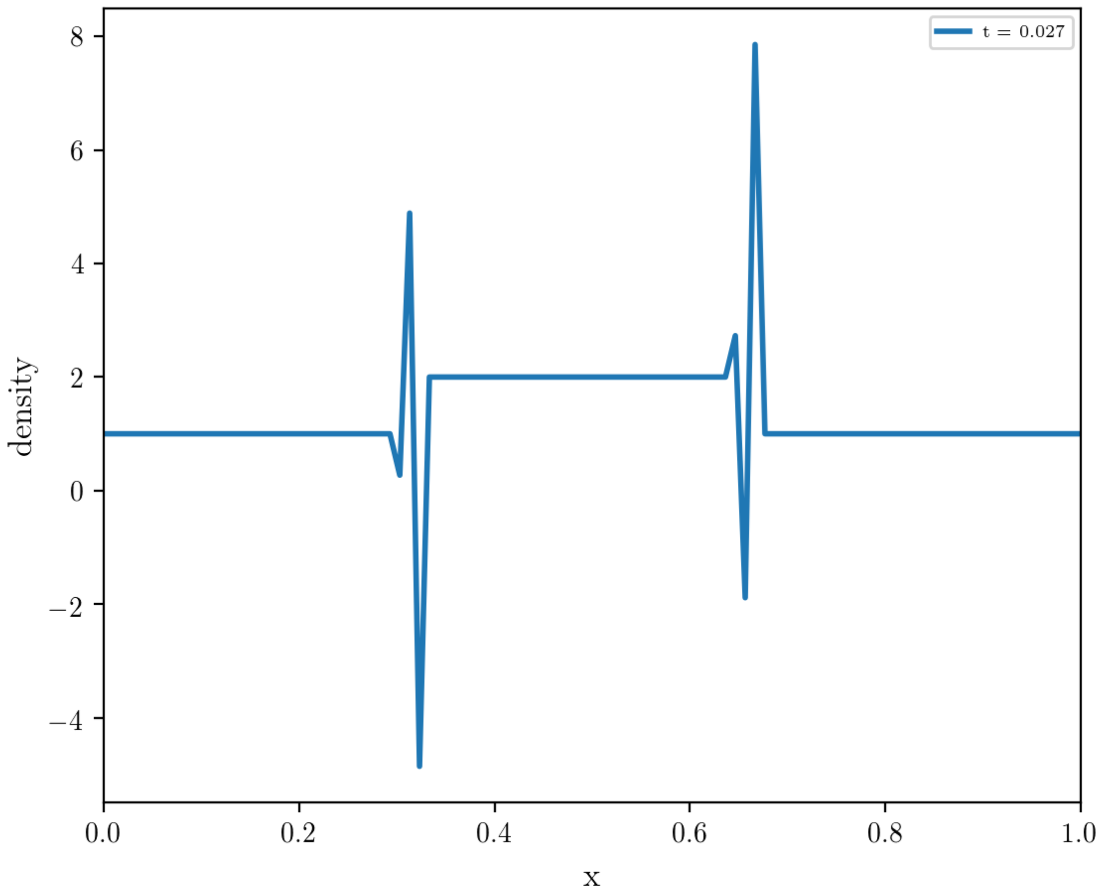

Figure 28: Downwind differencing after 3 steps.

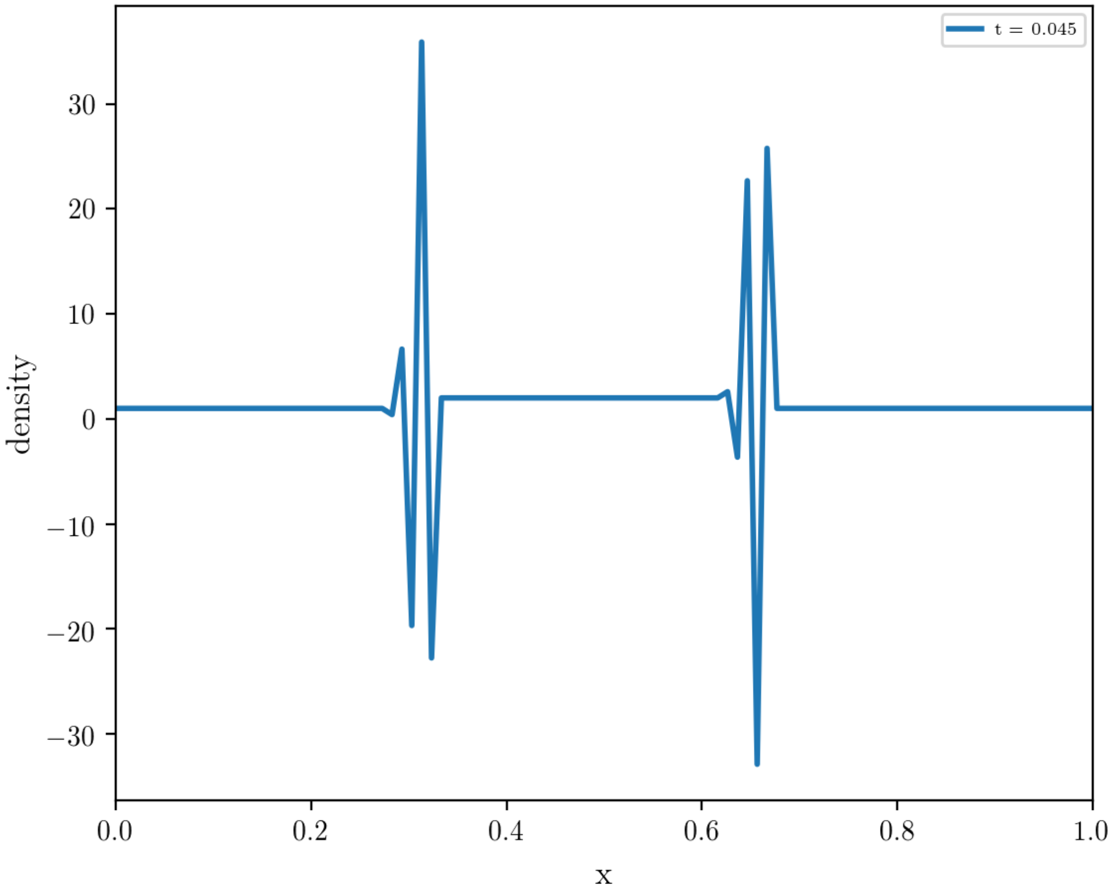

Figure 29: Downwind differencing after 5 steps.

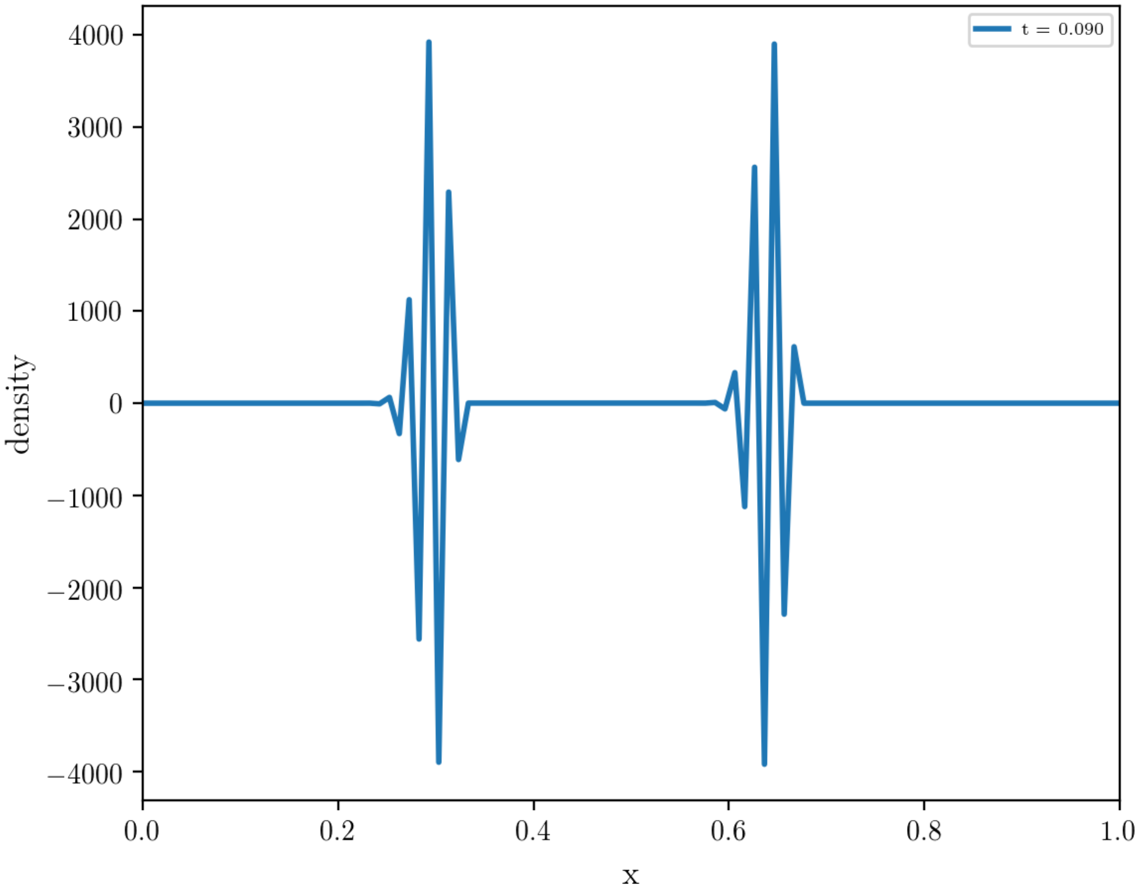

Figure 30: Downwind differencing after 10 steps.

2.5.2 When the CFL condition is violated

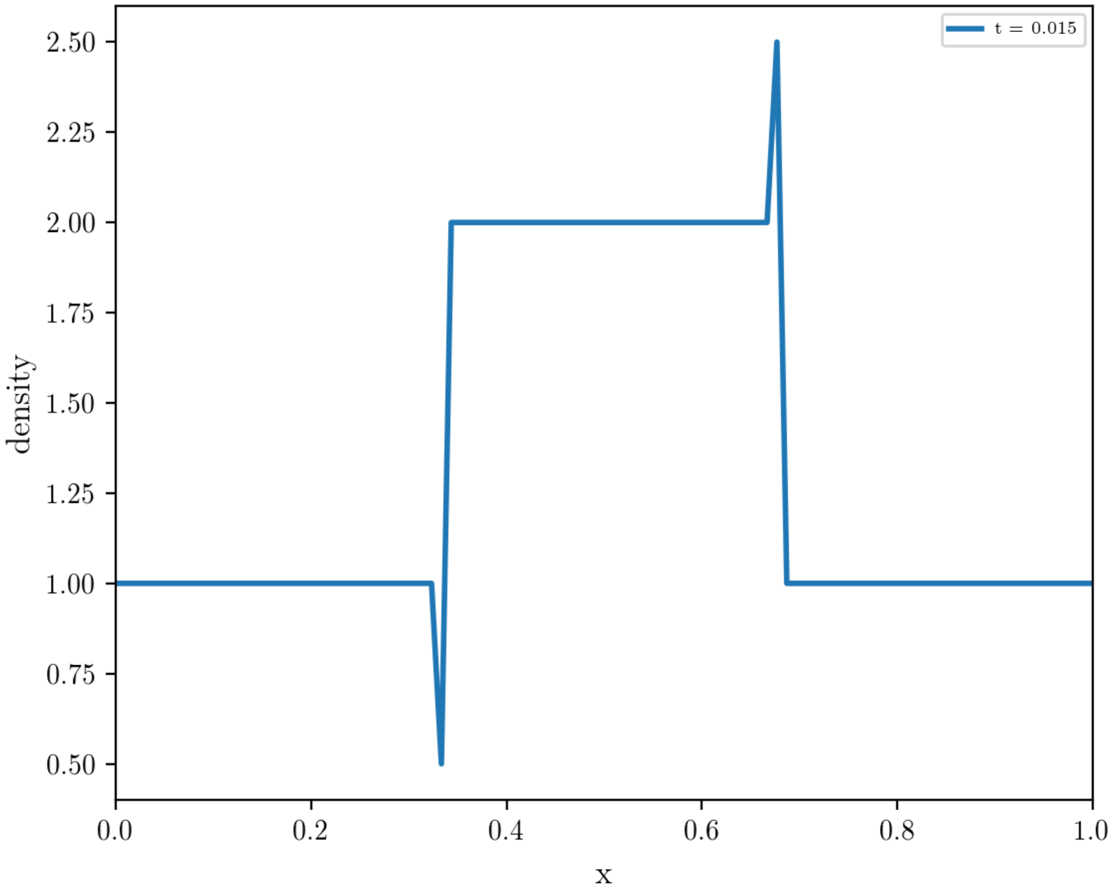

Figure 31: Violating the CFL condition (here $C_{cfl} = 1.5$) after 1 step.

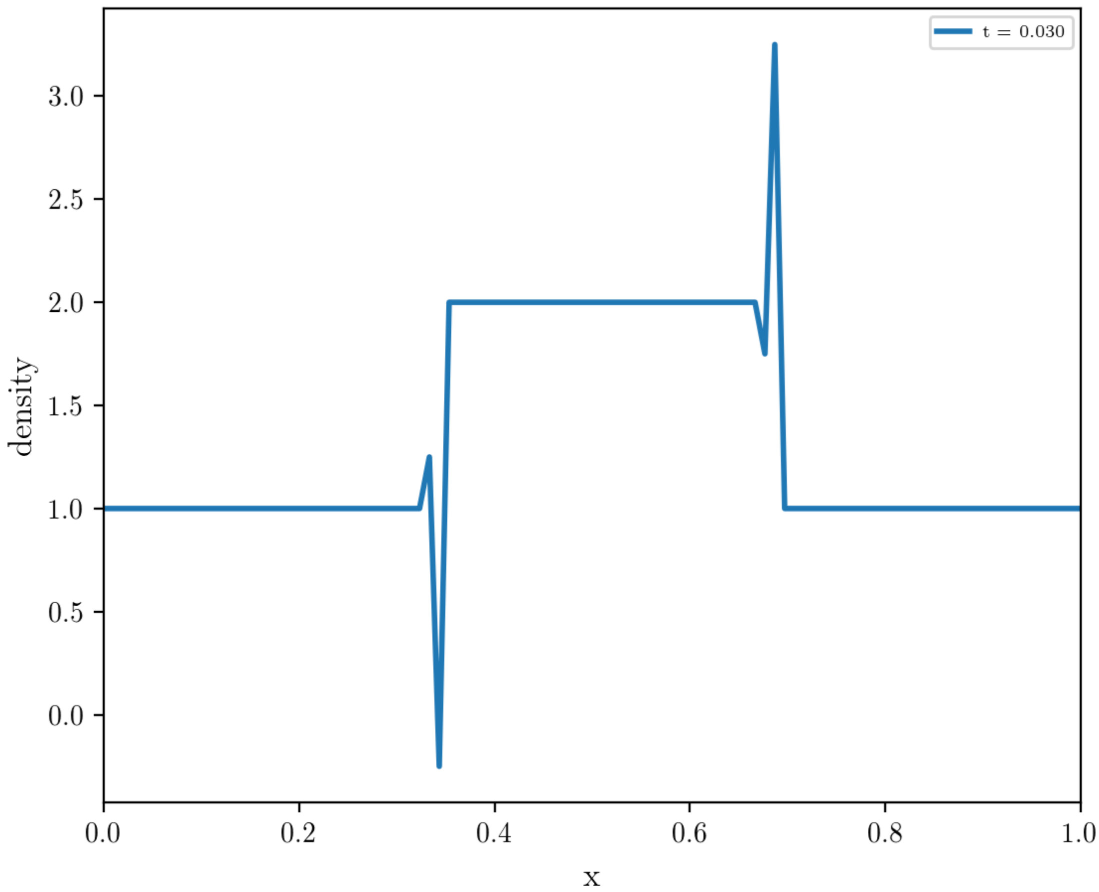

Figure 32: Violating the CFL condition (here $C_{cfl} = 1.5$) after 2 steps.

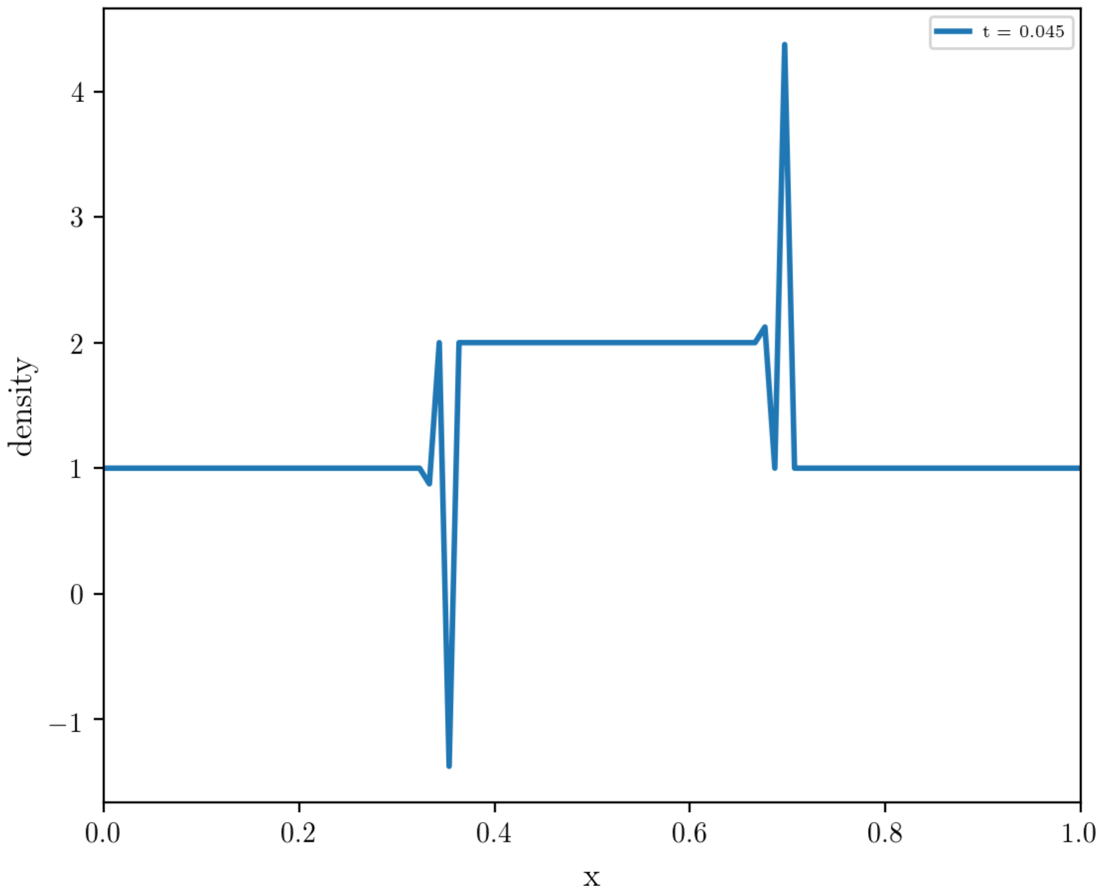

Figure 33: Violating the CFL condition (here $C_{cfl} = 1.5$) after 3 steps.

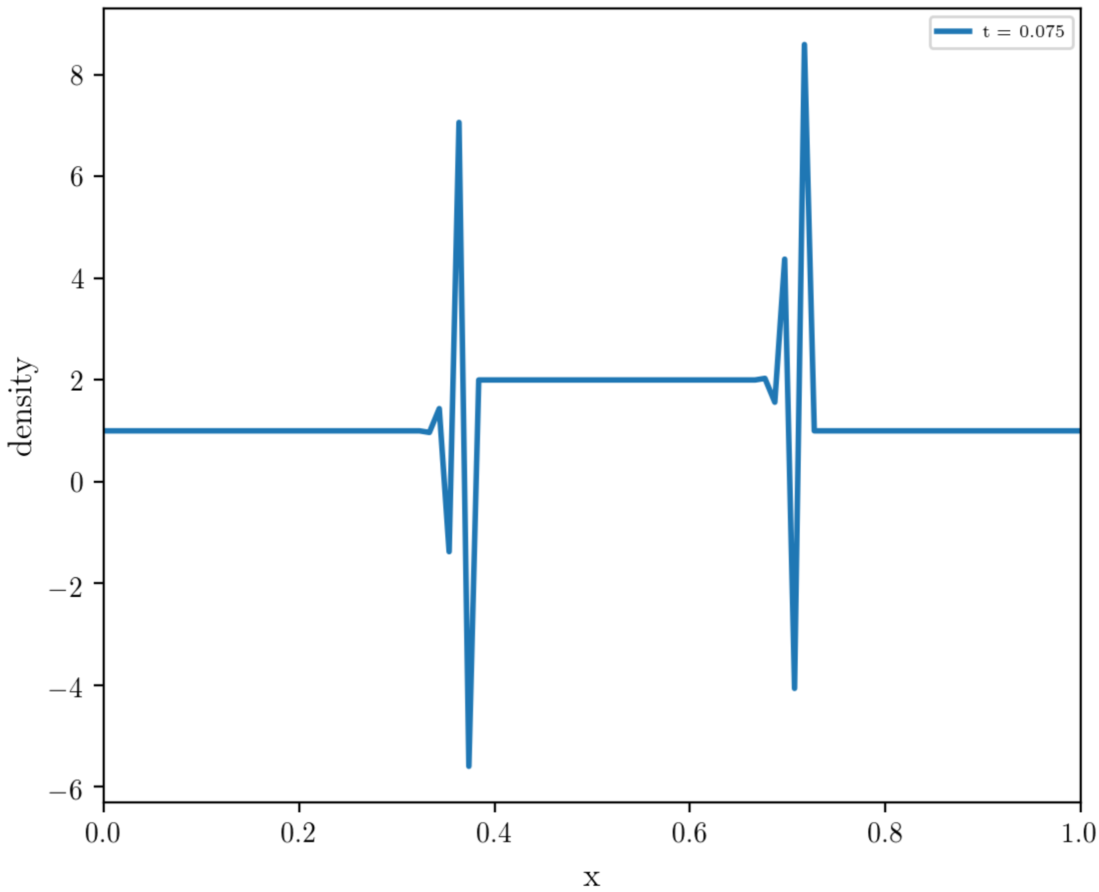

Figure 34: Violating the CFL condition (here $C_{cfl} = 1.5$) after 5 steps.

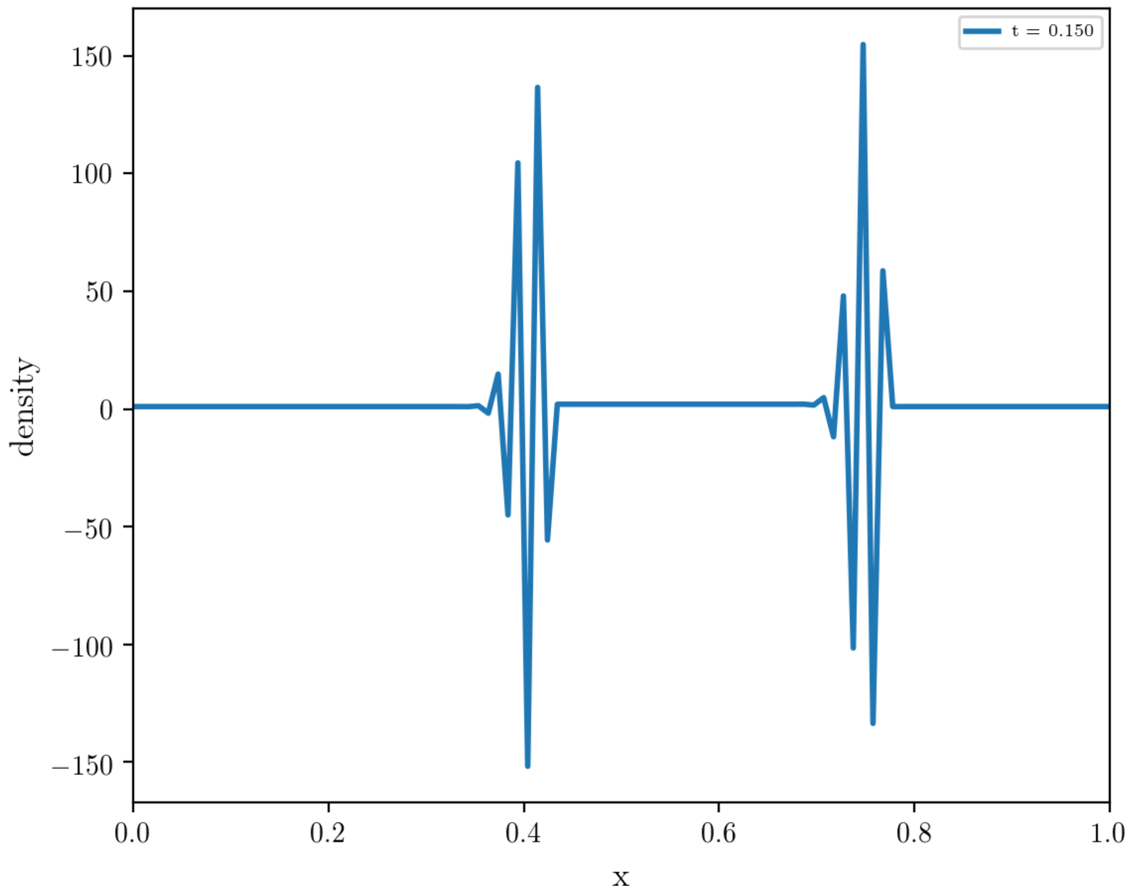

Figure 35: Violating the CFL condition (here $C_{cfl} = 1.5$) after 10 steps.

3 Slope and Flux Limiters

3.1 Slope Limiters

Slope limiters are employed because issues arise around numerical schemes because of their discrete nature. For example, a non-limited piecewise linear advection scheme will produce oscillations around jump discontinuities. See **Godunov's Theorem**:

> Linear numerical schemes for solving partial differential equations (PDE's), having the property of not generating new extrema (monotone scheme), can be at most first-order accurate.

So the idea is to compute the slope in way that is useful for us based on the current situation of the gas state that we're solving for.

The choice of the slope can be expressed via a function $\phi(r)$. For simple advection, we are solving the equation:

$$\mathbf{U}_i^{n+1} = \mathbf{U}_i^n + \frac{\Delta t}{\Delta x}\left(\mathbf{F}_{i-1/2}^{n+1/2} - \mathbf{F}_{i+1/2}^{n+1/2}\right) \tag{19}$$

If we assume that the states $\mathbf{U}_i$ are piecewise linear, i.e.

$$\mathbf{U}(\mathbf{x}) = \mathbf{U}_i(\mathbf{x}_i) + \mathbf{s}\cdot(\mathbf{x}-\mathbf{x}_i) \qquad \text{for } \mathbf{x}_{i-1/2} \leq \mathbf{x} \leq \mathbf{x}_{i+1/2} \tag{20}$$

then the expression for the fluxes is given by

$$\mathbf{F}_{i-1/2}^{n+1/2} = \begin{cases} \mathbf{v}_{i-1/2}\cdot\mathbf{U}_{i-1}^n + \frac{1}{2}\mathbf{v}_{i-1/2}\cdot\mathbf{s}_{i-1}^n(\Delta\mathbf{x} - \mathbf{v}_{i-1/2}\Delta t) & \text{for } \mathbf{v}\geq 0 \\ \mathbf{v}_{i-1/2}\cdot\mathbf{U}_{i}^n - \frac{1}{2}\mathbf{v}_{i-1/2}\cdot\mathbf{s}_{i}^n(\Delta\mathbf{x} + \mathbf{v}_{i-1/2}\Delta t) & \text{for } \mathbf{v}\leq 0 \end{cases}$$

$$\mathbf{F}_{i+1/2}^{n+1/2} = \begin{cases} \mathbf{v}_{i+1/2}\cdot\mathbf{U}_{i}^n + \frac{1}{2}\mathbf{v}_{i+1/2}\cdot\mathbf{s}_{i}^n(\Delta\mathbf{x} - \mathbf{v}_{i+1/2}\Delta t) & \text{for } \mathbf{v}\geq 0 \\ \mathbf{v}_{i+1/2}\cdot\mathbf{U}_{i+1}^n - \frac{1}{2}\mathbf{v}_{i+1/2}\cdot\mathbf{s}_{i+1}^n(\Delta\mathbf{x} + \mathbf{v}_{i+1/2}\Delta t) & \text{for } \mathbf{v}\leq 0 \end{cases}$$

We can now insert a more general expression for the slopes: Let

$$\theta_{i-1/2} = \begin{cases} +1 & \text{for } \mathbf{v} \geq 0 \\ -1 & \text{for } \mathbf{v} \leq 0 \end{cases} \tag{21}$$

Then

$$\begin{aligned} \Delta x_{i-\{0,1\}} \mathbf{s}_{i-\{0,1\}} &= \frac{1}{2} \Delta x \left[(1+\theta_{i-1/2}) \mathbf{s}_{i-1}^n + (1-\theta_{i-1/2}) \mathbf{s}_i^n \right] \qquad (22) \\ &\equiv \phi(r_{i-1/2}^n)(\mathbf{U}_i^n - \mathbf{U}_{i-1}^n) \qquad (23) \\ r_{i-1/2}^n &= \begin{cases} \frac{\mathbf{U}_{i-1}^n - \mathbf{U}_{i-2}^n}{\mathbf{U}_i^n - \mathbf{U}_{i-1}^n} & \text{for } \mathbf{v} \geq 0 \\ \frac{\mathbf{U}_{i+1}^n - \mathbf{U}_i^n}{\mathbf{U}_i^n - \mathbf{U}_{i-1}^n} & \text{for } \mathbf{v} \leq 0 \end{cases} \qquad (24) \end{aligned}$$

This defines ϕ, which will be discussed later. Finally:

$$\begin{aligned} \mathbf{F}_{i-1/2}^{n+1/2} =& \frac{1}{2} \mathbf{v}_{i-1/2} \left[(1+\theta_{i-1/2}) \mathbf{U}_{i-1}^n + (1-\theta_{i-1/2}) \mathbf{U}_i^n \right] + \\ & \frac{1}{2} |\mathbf{v}_{i-1/2}| \left(1 - \left| \frac{\mathbf{v}_{i-1/2} \Delta t}{\Delta x} \right| \right) \phi(r_{i-1/2}^n)(\mathbf{U}_i^n - \mathbf{U}_{i-1}^n) \qquad (25) \\ \mathbf{F}_{i+1/2}^{n+1/2} =& \frac{1}{2} \mathbf{v}_{i+1/2} \left[(1+\theta_{i+1/2}) \mathbf{U}_i^n + (1-\theta_{i+1/2}) \mathbf{U}_{i+1}^n \right] + \\ & \frac{1}{2} |\mathbf{v}_{i+1/2}| \left(1 - \left| \frac{\mathbf{v}_{i+1/2} \Delta t}{\Delta x} \right| \right) \phi(r_{i+1/2}^n)(\mathbf{U}_{i+1}^n - \mathbf{U}_i^n) \qquad (26) \end{aligned}$$

Depending on our choice of ϕ, we can get different slopes. Here for positive velocity only, and for $r = r_{i-1/2}$:

$\phi(r) = 0 \rightarrow \mathbf{s}_i = 0$	No slopes; Piecewise constant method.
$\phi(r) = 1 \rightarrow \mathbf{s}_i = \dfrac{\mathbf{U}_i - \mathbf{U}_{i-1}}{\Delta x}$	Downwind slope (Lax-Wendroff)
$\phi(r) = r \rightarrow \mathbf{s}_i = \dfrac{\mathbf{U}_{i-1} - \mathbf{U}_{i-2}}{\Delta x}$	Upwind slope (Beam-Warming)
$\phi(r) = \dfrac{1}{2}(1+r) \rightarrow \mathbf{s}_i = \dfrac{\mathbf{U}_i - \mathbf{U}_{i-2}}{2\Delta x}$	Centered slope (Fromm)

Note that taking the downwind slope is very different from doing downwind differencing! We only use the downwind value to estimate the state inside the cell, not to compute derivatives.

As was said before, these kinds of slopes will introduce oscillations around jump discontinuities in the advected quantity. See Godunov's theorem and figure 11.

3.1.1 What slope limiters have in common

So the idea behind slope limiters is to find an expression to **monotonize** the states, i.e. to be **Total Variation Diminishing (TVD)**. A method is TVD if:

$$TV(\mathbf{U}^n) \equiv \sum_j |\mathbf{U}_{j+1} - \mathbf{U}_j| \tag{27}$$

$$TV(\mathbf{U}^{n+1}) \leq TV(\mathbf{U}^n) \quad \Leftrightarrow \quad \text{method is TVD} \tag{28}$$

Remember, we express the slopes with the function $\phi(r)$, where

$$r^n_{i-1/2} = \begin{cases} \frac{\mathbf{U}^n_{i-1} - \mathbf{U}^n_{i-2}}{\mathbf{U}^n_i - \mathbf{U}^n_{i-1}} & \text{for } \mathbf{v} \geq 0 \\ \frac{\mathbf{U}^n_{i+1} - \mathbf{U}^n_i}{\mathbf{U}^n_i - \mathbf{U}^n_{i-1}} & \text{for } \mathbf{v} \leq 0 \end{cases}$$

.

r is the ratio of the slopes, a measure of the "curvature", or "monotonicity" in that place. To remove oscillations, we want to go back to a first order expression (piecewise constant expression) when we find an oscillation, i.e. when the numerator and denominator have different signs. We get the piecewise constant expression for $\phi(r) = 0$

$\Rightarrow$ For slope limiters, we must have $r < 0 \Rightarrow \phi = 0$

Other restrictions follow from the constraint that the method should be TVD and continuous (see Sweby 1984):

$$
\begin{aligned}
r \leq & \phi(r) \leq 2r & & 0 \leq r \leq 1 & (29) \\
1 \leq & \phi(r) \leq r & & 1 \leq r \leq 2 & (30) \\
1 \leq & \phi(r) \leq 2 & & r > 2 & (31) \\
& \phi(1) = 1 & & & (32) \\
& & & & (33)
\end{aligned}
$$

Effectively, this defines regions in the $r - \phi(r)$ diagram through which the limiters are allowed to pass such that they are still TVD (fig 36)

Popular limiters are:

$$
\begin{aligned}
\text{Minmod} \qquad & \phi(r) = \text{minmod}(1, r) & (34) \\
\text{Superbee} \qquad & \phi(r) = \max(0, \min(1, 2r), \min(2, r)) & (35) \\
\text{MC (monotonized cenral-difference)} \qquad & \phi(r) = \max(0, \min((1+r)/2, 2, 2r)) & (36) \\
\text{van Leer} \qquad & \phi(r) = \frac{r + |r|}{1 + |r|} & (37)
\end{aligned}
$$

where

$$
\text{minmod}(a, b) = \begin{cases} a & \text{if } |a| < |b| \text{ and } ab > 0 \\ b & \text{if } |a| > |b| \text{ and } ab > 0 \\ 0 & \text{if } ab \leq 0 \end{cases} \tag{38}
$$

Their behaviour is shown in fig. 36.

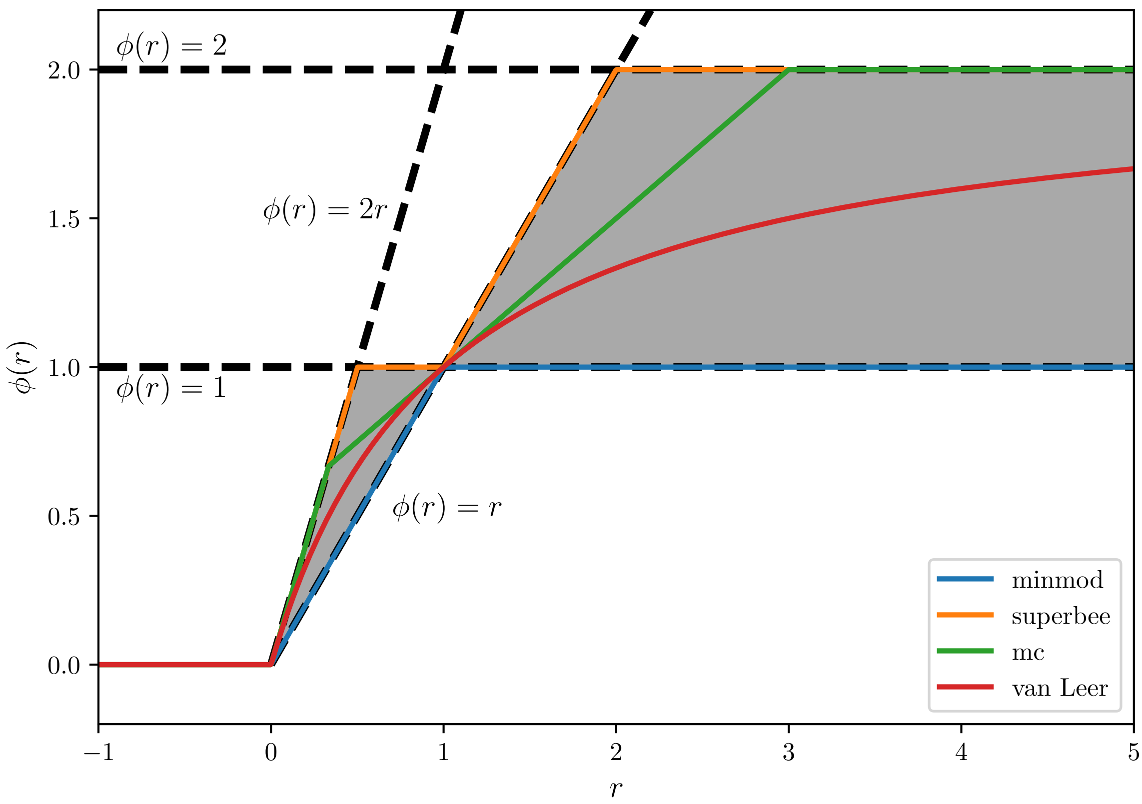

Figure 36: The behaviour for different slope limiters. The grey zone is the zone allowed by the conditions 29 - 31.

3.1.2 Effects on linear advection

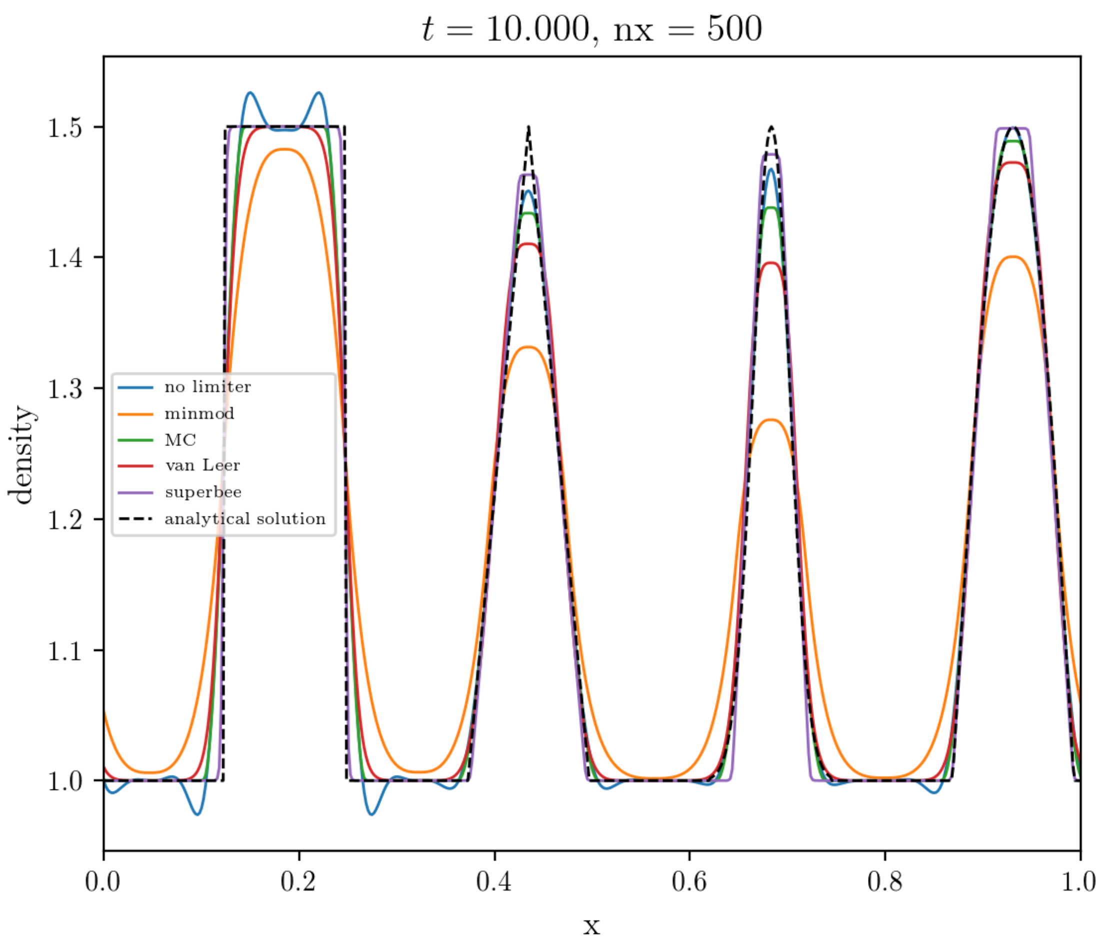

Figure 37: The effect of different slope limiters on linear advection, applied to piecewise linear advection (eqns 19, 20)

- All limiters except superbee still contain diffusion. You can't get rid of it entirely, but we got rid of the oscillations.
- The minmod resembles the solution of the piecewise constant advection, but pay attention that this is at much later times!
- Some limiters flatten continuous maxima. Van leer, then MC, then superbee in order of ascending "flattening"
- It's as if superbee tries to produce jump discontinuities

- For order of convergence study, see figs. 19 - 24, and discussion in section 2.4.

4 Riemann Solvers

4.1 Approximate Riemann Solutions

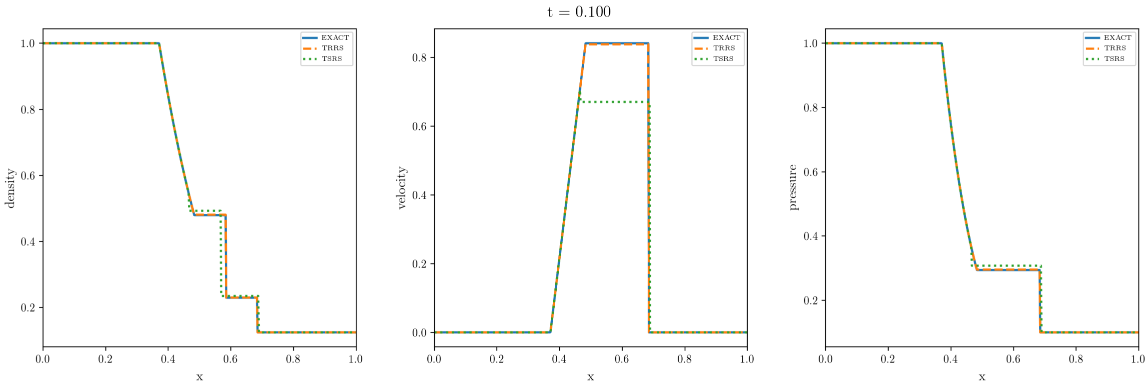

Figure 38: The Sod test solved using the exact and approximate Riemann solvers

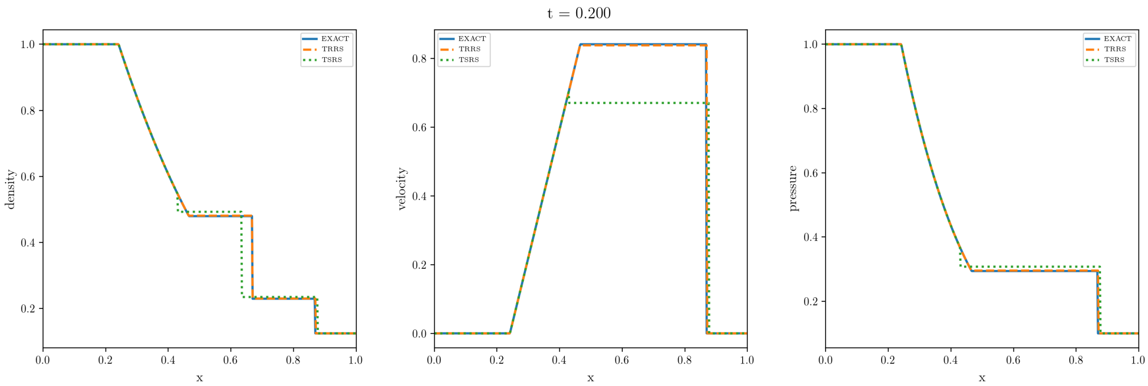

Figure 39: The Sod test solved using the exact and approximate Riemann solvers, at a later time

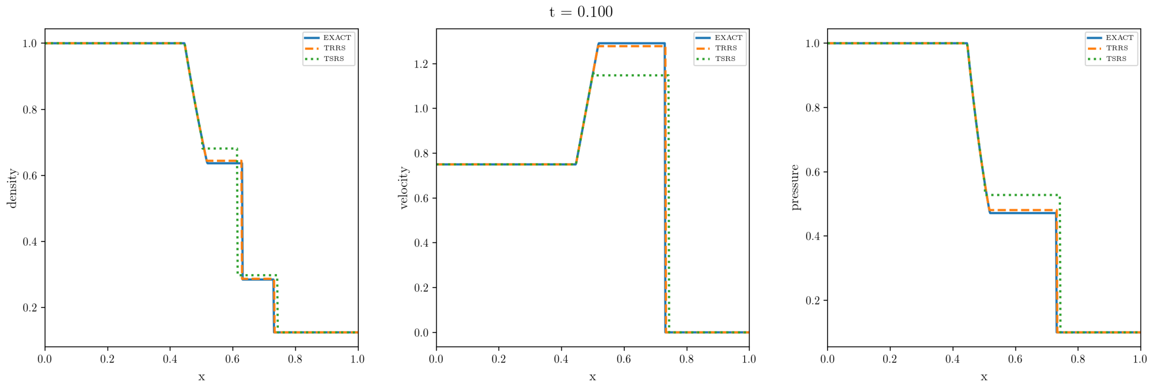

Figure 40: The modified Sod test solved using the exact and approximate Riemann solvers

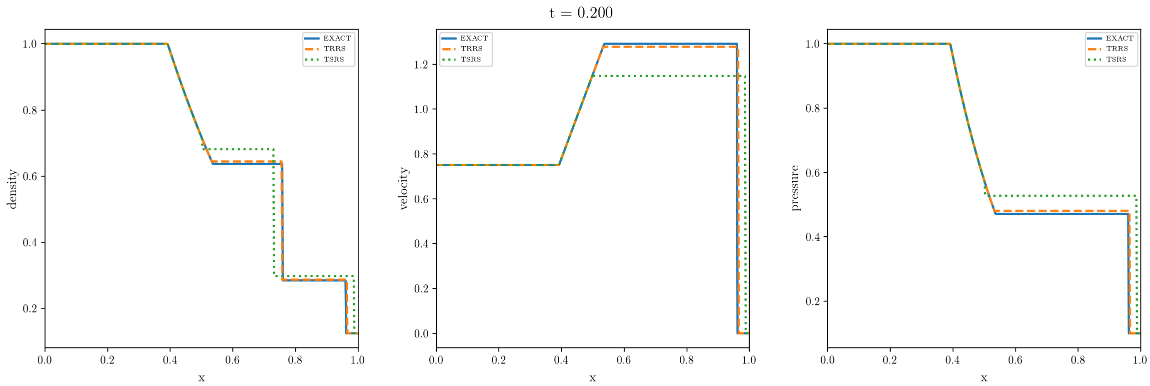

Figure 41: The modified Sod test solved using the exact and approximate Riemann solvers, at a later time

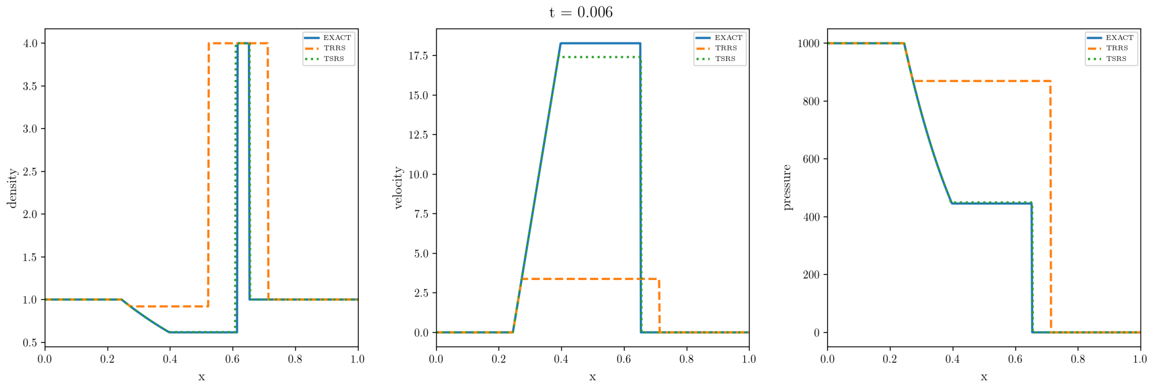

Figure 42: The left blast wave solved using the exact and approximate Riemann solvers

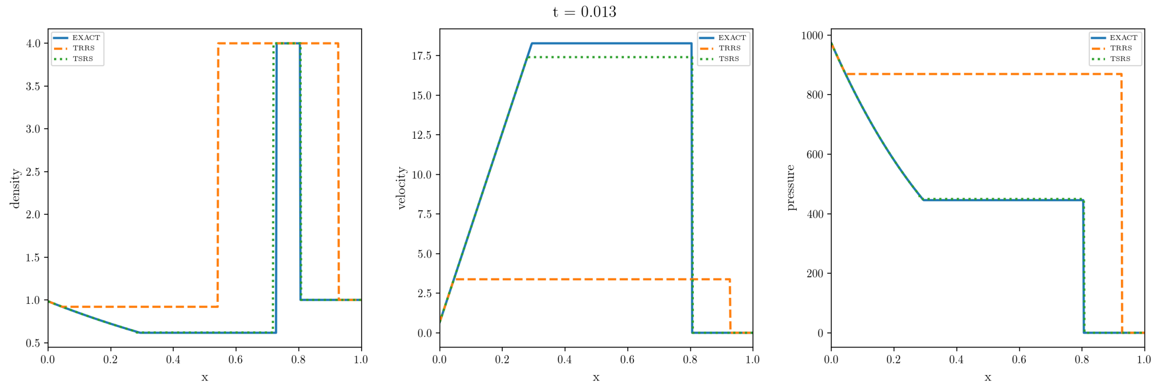

Figure 43: The left blast wave solved using the exact and approximate Riemann solvers, at a later time

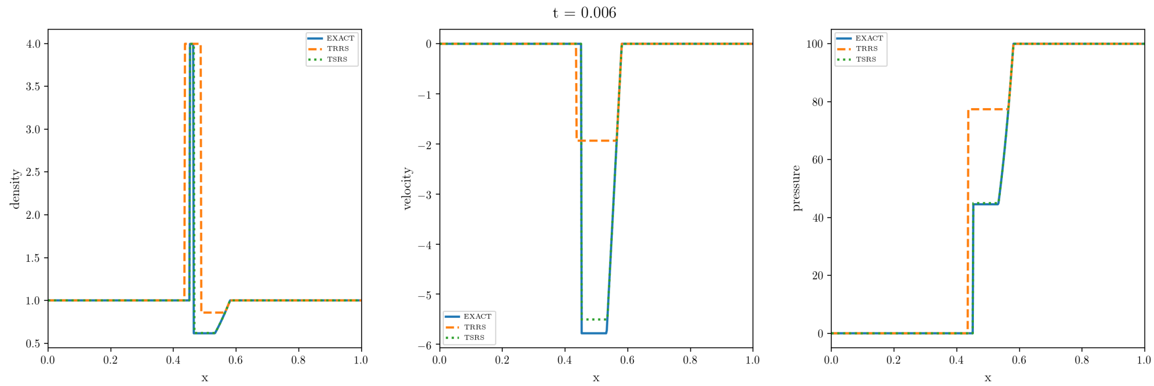

Figure 44: The left blast wave solved using the exact and approximate Riemann solvers

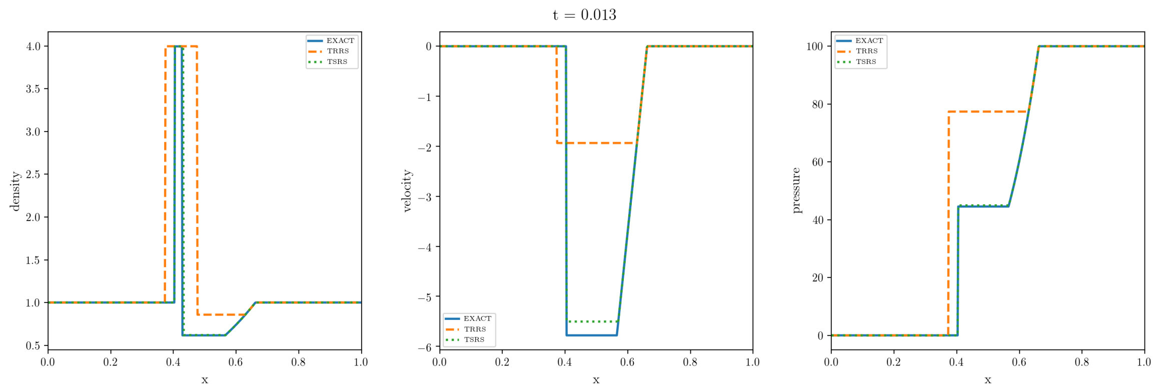

Figure 45: The left blast wave solved using the exact and approximate Riemann solvers, at a later time

4.2 Conclusions

- The TSRS solver may have trouble with rarefactions, e.g. figs 38 - 41. Which is to be expected, since it assumes that we have two shocks present. It deals much better with shocks, e.g. figs 42 - 45.
- The TRRS solver may have trouble with shocks, e.g. figs 42 - 45. Which is to be expected, since it assumes that we have two rarefactions present. It deals much better with rarefactions, e.g. figs 38 - 41.
- It looks like the results get worse over time. Compare figs 38 vs 39, 40 vs 41, etc. But recall that for the Riemann solver, we only solve the solution once, and then sample the solution for a given x and t. So once the four regions are determined initially, all the solver does is "smear them out" while sampling at a later time t.

5 Godunov's Method

5.1 Solving Riemann Problems using Godunov's Method

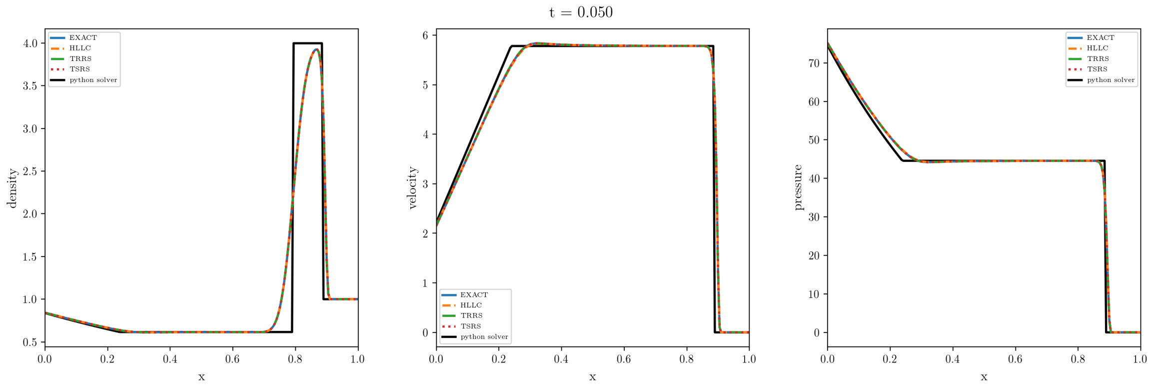

Figure 46: Solution to the left blast wave Riemann problem using Godunov's method and various Riemann solvers. The black line is the exact solution.

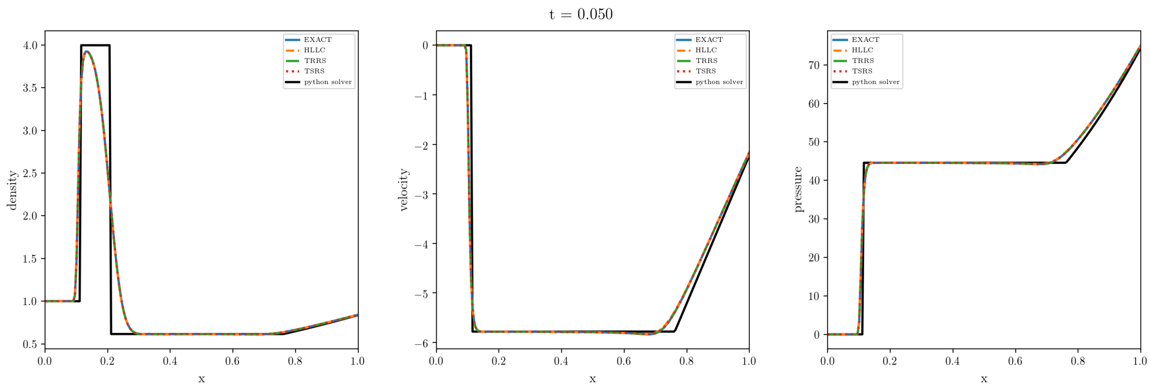

Figure 47: Solution to the right blast wave Riemann problem using Godunov's method and various Riemann solvers. The black line is the exact solution.

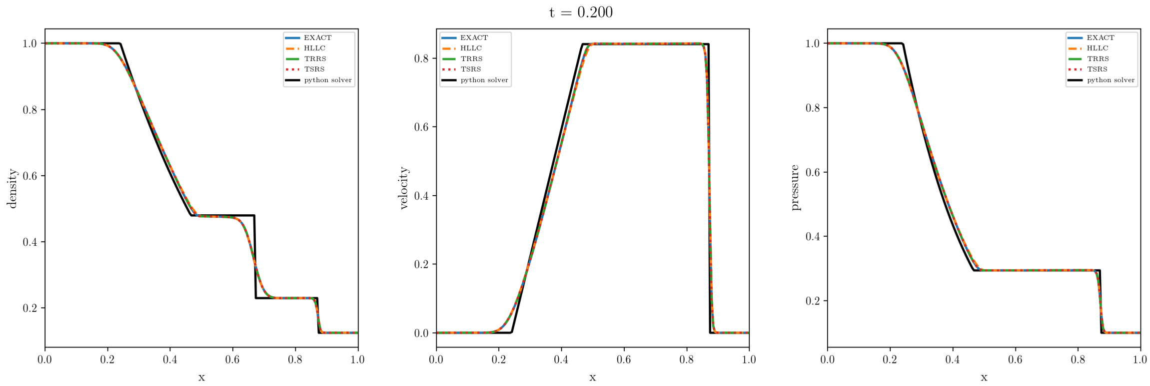

Figure 48: Solution to the sod test Riemann problem using Godunov's method and various Riemann solvers. The black line is the exact solution.

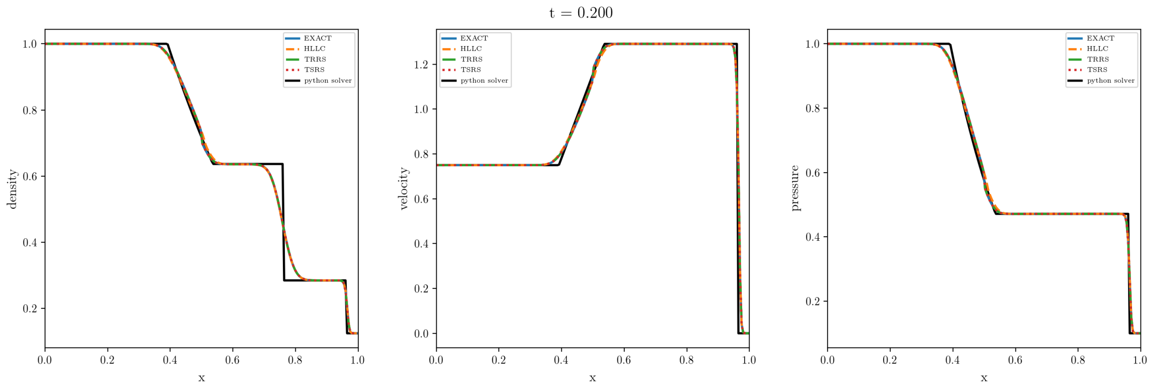

Figure 49: Solution to the modified sod test Riemann problem using Godunov's method and various Riemann solvers. The black line is the exact solution.

5.2 Solving Vacuum Riemann Problems using Godunov's Method

5.3 Order of Convergence Study

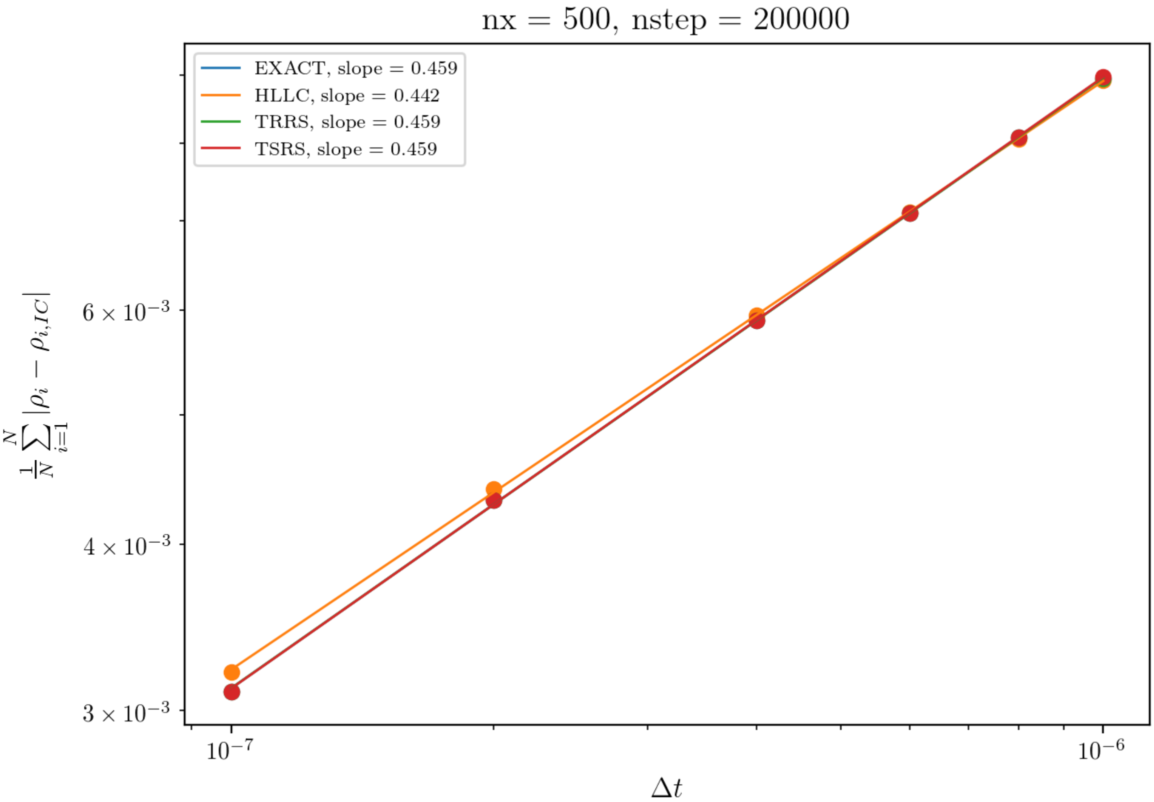

Figure 50: Testing the method's convergence with respect to the time step Δt on Sod test initial conditions. For a fair comparison, both the cell width Δx and the number of steps taken are fixed. The points are measurements, the lines are a linear fit, with the slope of the line given in the legend for each Riemann solver used in the legend.

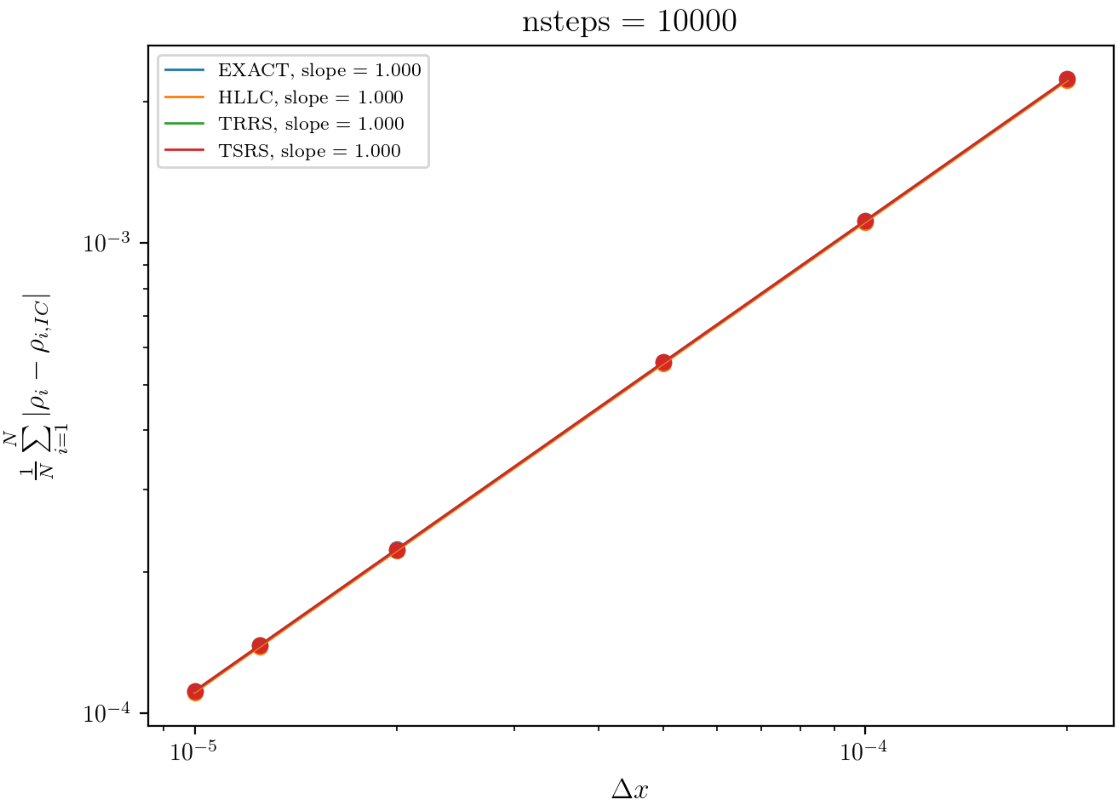

Figure 51: Testing the method's convergence with respect to the cell width Δx on Sod test initial conditions. For a fair comparison, the Courant number C_{CFL} and the total number of steps are fixed. The points are measurements, the lines are a linear fit, with the slope of the line given in the legend for each Riemann solver used in the legend.

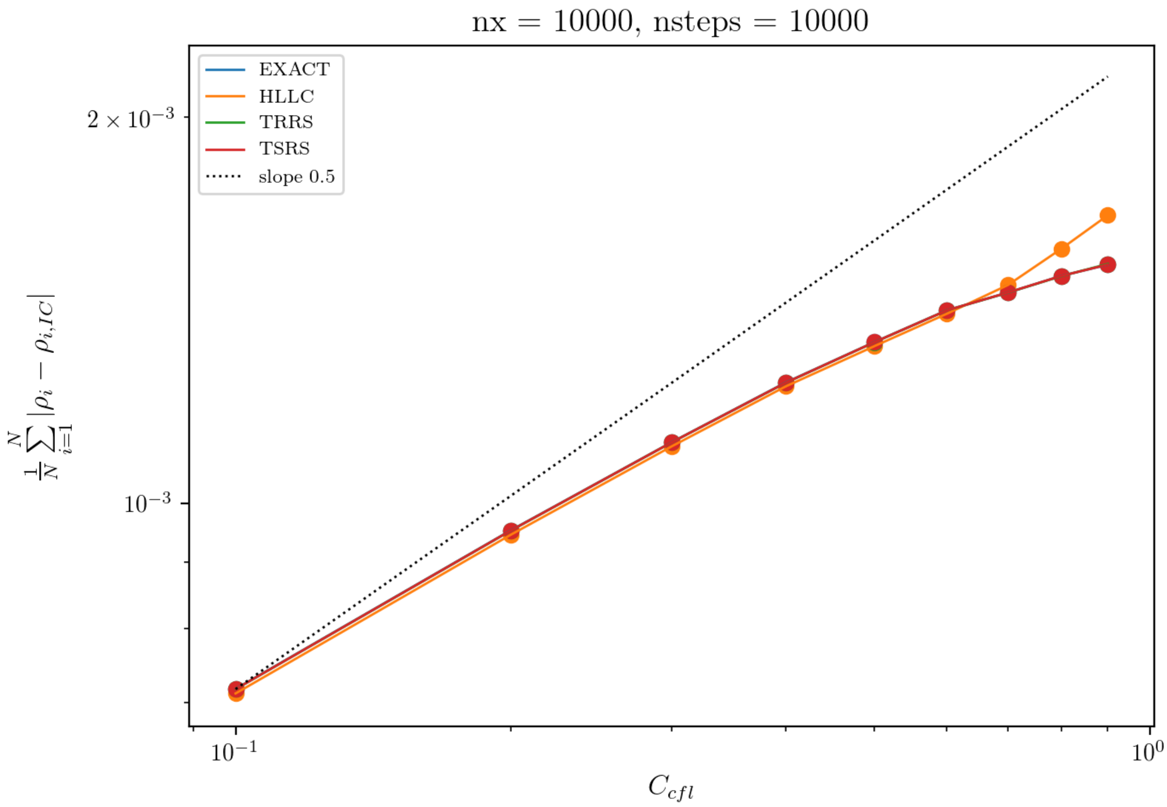

Figure 52: Testing the method's convergence with respect to the Courant number C_{CFL} on Sod test initial conditions. The points are measurements, the lines are just connecting them. The slope of 1/2 is plotted for comparison, and to demonstrate the deviation from it.

5.4 Conclusions

- Similar to the piecewise constant advection, the method is diffusive around sharp jump discontinuities. See figs. 46 - 49.
- **Order of Convergence**
  - Looking at the time step dependence (fig. 50), we always get slopes around ~ 0.5. Considering that a Sod test contains multiple jump discontinuities, this is absolutely as expected if we follow the same argumentation as for linear advection. See eq. 18 and derivation leading up to it for comparison. All in all, it remains true that jump discontinuities reduce the order of convergence w.r.t. the time step.
  - For the cell width dependence (fig. 51), we get a remarkable slope of 1.000

for all solvers. Even more remarkable, all the $L1$ norms are identical. No approximate solver introduces more or less errors in this test case.

- For the C_{cfl} dependence, we see that it deviates more stronger for higher C_{CFL} from the 0.5 power law that we get for small Δt. However, it is significantly better than what we get for advection (fig. 24).

  Why?

  Well, we don't necessarily have constant time steps any more, nor do we have constant velocities. It is conceivable that the errors "correct themselves" by demanding/allowing a smaller/larger timestep.

  What also might decrease the accuracy for high C_{cfl} is that I don't properly compute the emerging wave speeds, but estimate them; So there is a possibility that for high C_{cfl}, things are just computed wrongly, i.e. the chosen time step is too large to be stable or accurate.

References

[1] Randall J. LeVeque. *Finite Volume Methods for Hyperbolic Problems*. Cambridge Texts in Applied Mathematics. Cambridge University Press, 2002. DOI: 10.1017/CBO9780511791253.

[2] P. K. Sweby. "High Resolution Schemes Using Flux Limiters for Hyperbolic Conservation Laws". en. In: *SIAM Journal on Numerical Analysis* 21.5 (Oct. 1984), pp. 995–1011. ISSN: 0036-1429, 1095-7170. DOI: 10.1137/0721062.